Pergamon

Neuroscience Vol. 92, No. 2, pp. 407–426, 1999

PII: S0306-4522(98)00755-6
0306-4522/99 $20.00+0.00

HIGH-FREQUENCY POPULATION OSCILLATIONS ARE PREDICTED TO OCCUR IN HIPPOCAMPAL PYRAMIDAL NEURONAL NETWORKS INTERCONNECTED BY AXOAXONAL GAP JUNCTIONS

R. D. TRAUB,*† D. SCHMITZ,‡ J. G. R. JEFFERYS* and A. DRAGUHN‡

*Division of Neuroscience, University of Birmingham School of Medicine, Edgbaston, Birmingham B15 2TT, U.K.

‡Institut für Physiologie der Charité, Humboldt-Universität zu Berlin, Tucholskystraße 2, 10117 Berlin, Germany

Abstract—In hippocampal slices, high-frequency (125–333 Hz) synchronized oscillations have been shown to occur amongst populations of pyramidal neurons, in a manner that is independent of chemical synaptic transmission, but which is dependent upon gap junctions. At the intracellular level, high-frequency oscillations are associated with full-sized action potentials and with fast prepotentials. Using simulations of two pyramidal neurons, we previously argued that the submillisecond synchrony, and the rapid time-course of fast prepotentials, could be explained, in principle, if the requisite gap junctions were located between pyramidal cell axons. Here, we use network simulations (3072 pyramidal cells) to explore further the hypothesis that gap junctions occur between axons and could explain high-frequency oscillations. We show that, in randomly connected networks with an average of two gap junctions per cell, or less, synchronized network bursts can arise without chemical synapses, with frequencies in the experimentally observed range (spectral peaks 125–182 Hz). These bursts are associated with fast prepotentials (or partial spikes and spikelets) as observed in physiological recordings. The critical assumptions we must make for the oscillations to occur are: (i) there is a background of ectopic axonal spikes, which can occur at low frequency (one event per 25 s per axon); (ii) the gap junction resistance is small enough that a spike in one axon can induce a spike in the coupled axon at short latency (in the model, a resistance of 273 MΩ works, with an associated latency of 0.25 ms).

We predict that axoaxonal gap junctions, in combination with recurrent excitatory synapses, can induce the occurrence of high-frequency population spikes superimposed on epileptiform field potentials. © 1999 IBRO. Published by Elsevier Science Ltd.

Key words: electrotonic coupling, oscillations, epilepsy, ripples, graph theory.

This paper addresses the question: how might gap junctions contribute to the generation and shaping of high-frequency (>100 Hz) neuronal population oscillations in the hippocampus? In particular: could gap junctions determine the synchronization, and—if so—why does the population oscillate at one frequency and not another? Our network models contain pyramidal cells but no interneurons. Each pyramidal cell has multiple soma/dendritic compartments and a length of axon. Gap junctions are present between some pairs of axons. We shall not simulate ephaptic interactions produced by field effects. In some simulations, chemical synaptic excitatory synapses between pyramidal neurons were modelled as well as gap junctions; in the absence of interneurons in our model, this case would correspond (approximately) to an experiment with $GABA_A$ receptors blocked.

High-frequency oscillations have been recorded in the hippocampus under three conditions.

(1) Epileptiform field potentials *in vitro*, under conditions where synaptic transmission (at least excitatory) is intact. The epileptiform field potential, corresponding to synchronized bursting in a population of pyramidal neurons, has a slow component that lasts some tens of milliseconds; there is, additionally, a high-frequency component of population spikes at about 150–300 Hz, observable both in CA1 and in CA3.[25,49] In CA3, the slow component is positive in the stratum pyramidale and negative in strata radiatum and oriens; the high-frequency component has maximum amplitude in the stratum pyramidale.[32] In CA3, the high-frequency population spikes are aligned with action potentials in pyramidal cells; small transmembrane depolarizations, with intracellular negativity relative to a distant ground electrode, can occur just prior to the action potential, arguing for the possibility that electric field effects (resulting from current flows in the extracellular space, across membranes and through cells) contribute to the synchronization of firing.[27]

†To whom correspondence should be addressed.

Abbreviations: AHP, afterhyperpolarization; $[Ca^{2+}]_o$, extracellular Ca^{2+} concentration; EPSC, excitatory postsynaptic current; IS, initial segment.

Computer simulations that modelled pyramidal cells embedded in a three-dimensional resistive lattice (representing the extracellular space) were consistent with this interpretation.[39] The high-frequency component of the epileptiform field potential is not restricted to disinhibition models of epileptogenesis, but can occur in other models as well, including low extracellular Mg^{2+} concentration.[42] High-frequency (>100 Hz) electroencephalogram activity, recorded with subdural electrodes and lasting for several seconds, has also been seen at the onset of focal seizures in human patients (having complex partial seizures and tonic seizures of the supplementary motor type).[11]

So-called d-spikes or spikelets (depolarizing potentials a few millivolts in amplitude, of abrupt onset and slower decay) have been reported in CA1 pyramidal cells, during epileptogenesis induced by the $GABA_A$ receptor-blocking antibiotic penicillin.[25,26] Such potentials are presumably not initiated in the soma.[29] Schwartzkroin and Prince[25,26] also reported the occurrence of action potentials of abrupt onset from baseline, sometimes with inflections on the rising phase: these features are indicators of spike initiation at a site remote from the soma, perhaps in the axon.[30,31,37]

(2) High-frequency population spikes under conditions where chemical synapses are blocked. Runs of population spikes can also occur during so-called field bursts *in vitro*, during which synaptic transmission is blocked, although the frequency tends to be less than 100 Hz[12,14,33] (however, see fig. 1C of Ref. 21 for an example where the frequency is >100 Hz). The amplitude of the population spikes is maximal in the stratum pyramidale. Both Taylor and Dudek[34,35] and Haas and Jefferys[12] suggested field effects as a synchronizing mechanism, and, again, computer simulations were consistent.[40] Perez Velazquez *et al.*[23] noted, however, that blockers of gap junctional conductance (octanol, halothane, intracellular acidification) suppressed field bursts, while intracellular alkalinization—which enhances gap junctional conductance—increased the frequency and duration of field bursts; for such reasons, these authors suggested that gap junctions between pyramidal cells might be responsible for the synchronous firing characteristic of field bursts. The existence of gap junctions between somatic/dendritic membranes of adult pyramidal cells, derived from normal animals, remains somewhat problematic (but see Ref. 24). Taylor and Dudek[33] recorded partial spikes (10–20 mV) during field bursts, while Perez Velazquez *et al.*[23] and Valiante *et al.*[47] recorded spikelets in low extracellular Ca^{2+} ($[Ca^{2+}]_o$) media, the frequency of which was enhanced by intracellular alkalinization (with NH_4Cl). These data suggest that the occurrence of spikelets might be dependent, in some way, on gap junctions.

Draguhn *et al.*,[7] using hippocampal slices, showed that >100 Hz oscillations could occur as brief runs in the presence of normal extracellular media; the runs were enhanced (in incidence and duration) when excitability was increased. One effective means of increasing excitability consisted of bathing the slice in nominally zero $[Ca^{2+}]_o$ media, thereby simultaneously blocking synaptic transmission. The spontaneous high-frequency oscillations were of maximum amplitude in the stratum pyramidale and were synchronized over more than a hundred micrometres. As for field bursts, the spontaneous oscillations were suppressed, or enhanced, by treatments that, respectively, reduced or increased gap junctional conductances. Draguhn *et al.*[7] also observed spikelets in pyramidal neuron whole-cell recordings; by correlating intracellular and extracellular recordings, they showed that: (i) the field potential oscillation was multicellular in origin; and that (ii) a spikelet in one cell could be temporally aligned with a population spike, during which other cells were presumably firing full action potentials. Of 15 interneurons recorded, none participated in the spontaneous oscillations in a consistent way.

It is well known[1] that gap junctions between excitable cells tend to act as low-pass filters, so that potentials in the presynaptic neuron are smoothed (as well as reduced in amplitude) in the postsynaptic one. In a previous modelling study,[46] it was necessary to use a coupling ratio of nearly 0.5 in order for an action potential in one cell to induce an event in the other cell resembling a spikelet in time-course. In further simulations of a pair of pyramidal cells, using a much more accurate cell model,[41] Draguhn *et al.*[7] likewise observed smoothing of "presynaptic" potentials in an electrically coupled neuron, when a gap junction was located between homologous sites in the soma/dendritic membrane, but they noted that two electrotonically coupled neurons would behave quite differently when the gap junction was located between axons. In the latter case, a gap junction which produced an intersomatic coupling ratio of less than 0.05 could still allow an action potential to pass from the axon of one cell to the axon of the other cell, across the junction, because of the low-impedance load of the axons and because of the high axonal density of Na^+ channels. The action potential in the postsynaptic neuron could then propagate antidromically, and—if it blocked just distal to the axon intial segment—would induce a spikelet in the soma of the postsynaptic neuron. The postulate of axoaxonal gap junctions has anatomically verified precedents in neurobiology, including the mammalian retina,[48] between the Mauthner cell and commissural interneuron axons in fish,[51] and in the medullary pacemaker nucleus controlling electric organ discharge in weakly electric fish[9,36] (also see below).

(3) High-frequency "ripples" superimposed on the physiological sharp waves that occur *in vivo*, in the

hippocampus (CA1), retrohippocampal structures and the entorhinal cortex. Field potentials >100 Hz have been recorded in limbic structures during the occurrence of 50–100 ms physiological sharp waves.[3,4,52] Ripples are of maximal amplitude in the stratum pyramidale. About 15% of CA1 pyramidal cells fire during a rippling epoch, but generally a particular cell does not fire on each wave; on average, however, the action potentials that do occur are in phase with the ripple waves. Interneuron action potentials are time-locked to the waves, but with a phase delay. Ripple waves can be synchronized over distances as large as 5 mm in CA1. The waves are present in awake animals and in urethane-anaesthetized animals, but the gap junction-blocking anaesthetic halothane suppresses the ripples, while still allowing the physiological sharp waves to occur.[52]

In summary, there are a number of situations in the mammalian brain, especially the hippocampus, in which the excitability of pyramidal cells is increased (by excitatory synaptic input, lowered $[Ca^{2+}]_o$ or elevated extracellular K^+),[38] wherein synchronized high-frequency trains of pyramidal cell oscillations occur. The oscillations last from tens of milliseconds up to seconds (the latter in the case of seizures in humans). There is evidence that gap junctions are important for the oscillations to occur, both *in vitro* and with sharp wave-associated ripples *in vivo*. What determines the frequency of the oscillation is not at all clear, especially in those cases where synaptic transmission is blocked. For comparison, it is useful to consider an electrotonically coupled network in certain species of weakly electric fish.

The electric organ discharge of such fish runs continuously for the life of the fish, with frequencies of hundreds of hertz to over 1 kHz; the frequency is controlled with extraordinary stability and precision, although it is capable of behavioural modulation.[8,20] The signal controlling the electric organ discharge is generated in the medullary pacemaker nucleus, which is able to oscillate *in vitro* when it is disconnected from its normal extrinsic synaptic inputs. This nucleus contains 100–200 pacemaker neurons and a lesser number of relay cells; the function of the latter is to transmit the population oscillatory signal to the spinal cord. The pacemaker neurons are interconnected by gap junctions formed by axosomatic and axoaxonal (to initial segment) endings.[9,36] Under control conditions *in vitro*, the firing of pairs of pacemaker neurons is tightly time-locked, to within 0.25 ms; in the presence of halothane, however, even when the output of the pacemaker nucleus as a whole remains oscillatory, the tight phase relations between neuronal pairs are lost.[19] This suggests that gap junctions contribute to the synchronization. In addition, it may be that pacemaker neurons are capable of oscillating when disconnected from other pacemaker neurons.

EXPERIMENTAL PROCEDURES

Network structure

The network is similar to that employed by Traub *et al.*,[44] except that: (i) interneurons were not included; and (ii) some pairs of pyramidal cell axons could be coupled by a gap junction. The network consisted of 3072 pyramidal cells in a 96×32 cell array, with lattice spacing between cells of 20 μm. In addition, small networks of two, three or four neurons—interconnected by gap junctions—were also simulated.

Modelling a single pyramidal cell

Pyramidal cells were simulated using the model of Traub *et al.*[41] Each neuron contains 64 soma/dendritic compartments, an axon initial segment (IS) and four additional axonal compartments. Ionic conductances include, for soma/dendritic membranes, fast g_{Na}, high-threshold g_{Ca} (non-inactivating), delayed rectifier $g_{K(DR)}$, slow Ca^{2+}-dependent $g_{K(AHP)}$, and fast voltage- and Ca^{2+}-dependent $g_{K(C)}$; in the axon, only g_{Na} and $g_{K(DR)}$ were present, at densities of 500 and 250 mS/cm^2, respectively. R_{input} was 37.4 MΩ. Other electrotonic parameters included $R_m = 50{,}000$ Ω-cm^2 for soma/dendrites and 1000 Ω-cm^2 for the axon, $R_i = 200$ Ω-cm for the soma/dendrites and 100 Ω-cm for the axon, and $C_m = 0.75$ μF/cm^2 everywhere. The passive space constant of the axon was 0.16 mm. In this study, maximum g_{Ca} conductance was halved, relative to the original paper, to render the cells less prone to intrinsic bursting. Cells were depolarized with small somatic currents, 0.05–0.06 nA.

One property which these model neurons possess (and which has been shown experimentally to exist in rat CA3 pyramidal cells[41]) is that of reflected spikes: antidromic activation of the neuron can sometimes—owing to the somatic spike being significantly wider than the axonal spike—evoke a second spike in the axon that then propagates orthodromically. The interval between the two axonal spikes can be as short as 1.6 ms (625 Hz) in simulations. Reflected spikes may contribute to synchronous activity in the absence of synaptic transmission (see Results). In simulations of one cell, and of two axonally coupled cells, we have never seen spikes reflecting from the distal end of the axon: continuous reverberating activity is not generated by "axonal reflections".

Recurrent chemical excitatory synaptic connections, mediated by α-amino-3-hydroxy-5-methyl-4-isoxazolepropionate receptors, were simulated in some instances. Each pyramidal neuron received synaptic input from 30 other pyramidal cells, chosen randomly. Each synaptic connection consisted of a single contact onto a basilar dendritic compartment, and had unitary synaptic conductance of $0.75 \times t \times e^{-t/2}$ nS (t = time in ms) or of $1.5 \times t \times e^{-t/2}$ nS.

Simulated axoaxonic gap junctions between pairs of pyramidal cells

Gap junctions were placed between the penultimate axonal compartments of some pairs of pyramidal cells (Fig. 1). The penultimate compartment is centred 262.5 μm from the soma. Junctions were symmetric and non-rectifying. When the junctional resistance was 424 MΩ (conductance 2.36 nS), an action potential would not cross from one axon to the other, in simulations of neuronal pairs; crossing was possible when the junctional resistance was ≤ 382 MΩ (conductance ≥ 2.62 nS). In the simulations illustrated here, unless noted otherwise, we used a junctional resistance of 273 MΩ (conductance 3.66 nS). In a pair of axonally coupled model cells, this junctional resistance decreased R_{input} by 0.5% and produced a coupling ratio (as defined in Ref. 16) of 0.04. (In some network simulations, gap junctions were instead located in the axonal

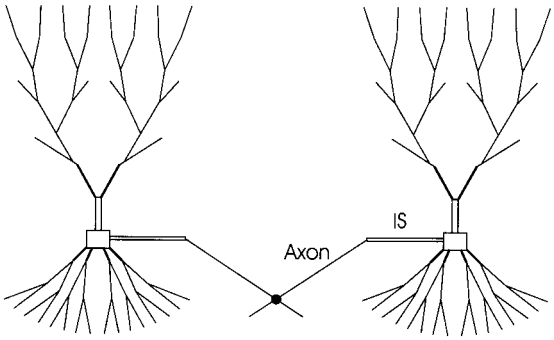

Fig. 1. Simulation of axoaxonal gap junctions. Diagram illustrating the structure of two model pyramidal cells joined by an axoaxonal gap junction. The structure of each cell is as in Ref. 41: a soma, 63 dendritic compartments, an initial segment (IS) and four additional unmyelinated axonal compartments. Junctions can form between the penultimate axonal compartments, centred at a distance $3.5 \times 75 = 262.5$ μm from the soma. Junctions are symmetrical and non-rectifying, and usually have a resistance of 273 MΩ (3.66 nS). Up to four axons can be joined at a single site. The average number of gap junctions per axon ranged between 0.95 and 3.0 in different network simulations.

compartment just distal to the IS, with results similar to those reported here.)

Networks of neurons interconnected sparsely by axoaxonic gap junctions

Electrotonic networks were formed by coupling (axon → axon) some of the neurons to other neurons. These networks were sparse, in that the number of cells contacted by any one cell was a tiny fraction of the whole system, at most four cells; some cells did not contact any other cells, i.e. they were "electrotonically isolated". These assumptions were made because Draguhn *et al.*[7] found many intracellularly recorded pyramidal cells that did not participate in high-frequency oscillations (the latter measured with field potential recordings). A distance constraint was imposed on the connectivity when the network was random (which corresponds, we believe, to the biological situation): for two cells to be electrotonically coupled, their respective somata had to lie within 200 μm of each other. [The resulting network is defined mathematically, but cannot, in general, be realized as such physically. To see this, consider cells c_1, c_2, …, c_5, where c_i and c_{i+1} somata are 150 μm apart, and the axons of c_i and c_{i+1} are coupled together ($i = 1, \ldots, 4$). The distance from c_1 to c_5 can be as large as 600 μm, but c_1's coupling site is 262.5 μm from its soma, as is true for c_5. This is not possible. To achieve physical realizability, one would have to, for example, allow the model neurons to have longer axons, or else to allow coupling between different sites on the axon—we await anatomical guidance on these issues.]

We simulated networks with two general sorts of connectivity (Fig. 2): binary trees and random. Binary trees are so highly structured as to be implausible as a faithful representation of a biological network, but trees have the advantages of: (i) being easily visualizable; and (ii) of having no cycles: the absence of cycles allows one to examine whether reentrant loops in the electrotonic network are necessary for population oscillations to occur. The particular binary tree that we used has 11 "levels", involving a total of 2047 neurons and 2046 gap junctions, so that the total number of junctions emerging from any one axon is $2 \times 2046/2047 = 1.999$ (recall that each gap junction interconnects two neurons, hence the factor of 2 in this equation). The remaining $3072 - 2047 = 1025$ neurons are electrotonically isolated. On the tree, the cells in level k ($k = 0, \ldots, 10$) are 2^k, …, $2^{k+1} - 1$. The cell L (> 1) has a "downward" junction to cell $L/2$ if L is even, or to $(L-1)/2$ if L is odd. If $L < 2^{10} = 1024$, then L has upward connections to cells $2 \times L$ and $2 \times L + 1$. This defines the topology of the tree.

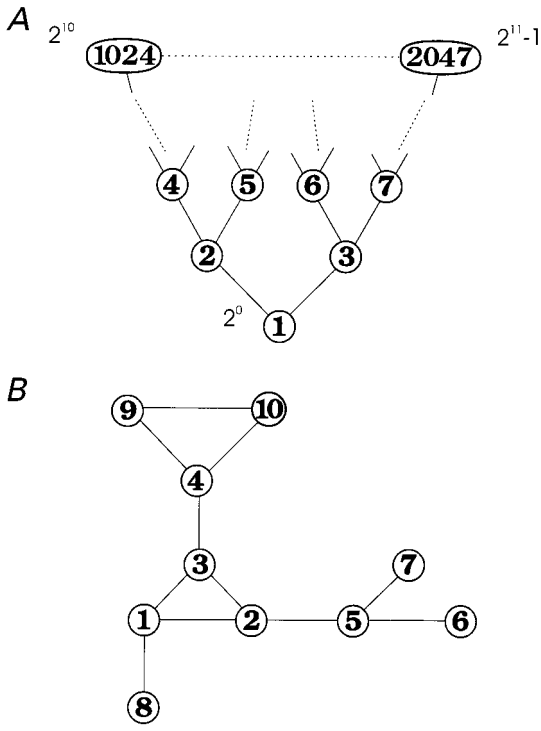

Fig. 2. Examples of graphs. (A) A binary tree with "root" at node 1, with 2047 nodes and 2046 branches, hence an average of 1.999 edges emerging from each node. There are no non-trivial cycles in this graph (an example of a trivial cycle would be 1 → 2 → 1). The mean path length between pairs of nodes is 16.04 ± 3.34. (B) A small graph with a more irregular structure, intended to give some of the flavour of a large random graph. There are 10 nodes and 10 edges, so that an average of two edges emerge from each node. There is a non-trivial cycle, the triangle. The mean path length is 2.64.

One way of characterizing the structure of a network, besides describing the cycles (or loops) in it, is with the average distance from one element to another, the mean path length. In this context, we do not mean physical distance, but rather how many junctions must be crossed to pass, within the network, from the first element to the second. This quantity is averaged over all possible pairs of elements. It is not difficult to calculate the mean path length using the computer; in the case of the 2047-cell binary tree, the mean path ($\pm$ S.D.) is 16.04 ± 3.34. If the latency for spread of action potentials from one axon to another is known, then the mean path length provides an estimate of oscillation intervals in the neuronal network (see below).

The other type of network simulated is random, or—to be more precise—random subject to two constraints: (i) physical distance between the somata of connected cells <200 μm; and (ii) total number of junctions formed by any one axon ≤ 4. We also require that at most one junction can form between any pair of axons. In order to construct such a network, we first specified the average number j of junctions formed on each axon. (We used values of j from 1.05 to 3.0 average junctions emerging from each axon.) Multiplying j by $3072/2 = 1536$ gives the total number n of junctions to be inserted into the network. Pairs of cells were generated successively, using a pseudo-random number generator, discarded if constraints (i) and (ii)

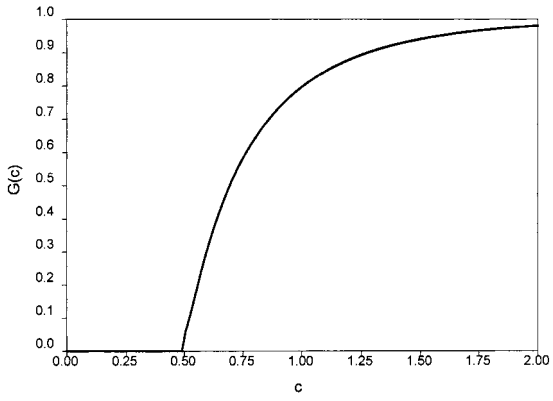

Fig. 3. Size of the largest cluster (as a fraction of total network size) as a function of mean connectivity, in the limit as network size approaches infinity. This graph is replotted from the function $G(c)$ (see text), derived by Erdös and Rényi,[10] using the first 250 terms of the infinite series, calculated at intervals of 0.005 for $c > 0.5$, the critical value. These authors considered randomly connected graphs with n nodes and N edges such that $N = cn$, and examined properties in the limit as n becomes unbounded. (The average number j of edges emerging from each node is $2 \times c$.) $G(c) =$ (number of nodes in largest cluster)/n. When $c < 0.5$ ($j < 1.0$), the largest cluster becomes vanishingly small, relative to the size of the network. When c is above 0.5 (j above 1.0), the largest cluster has a size of the same order as the network size, and it approaches network size asymptotically as the connectivity increases. All other clusters remain small relative to the whole network: there can be only one cluster whose size is comparable to that of the network.

above were not both met, and otherwise added to the system, until n junctions were formed. The large random networks that arise in this way are impossible to draw, but can be initially described in terms of the cluster distribution. Define a cluster of cells to be a set of cells with these two properties: (i) given a pair of cells in the set, one can pass from one cell to the other, either directly or else passing along junctions to intermediate cell(s) within the set; (ii) adding any additional cells to the set destroys property (i). In other words, a cluster is a set of cells that are connected together (directly or indirectly), but which cannot be made larger without losing connectedness. The overall network, then, will consist of some number of isolated cells, of pairs, triplets, 4-tuples, …, n-tuple(s), where $n \leq 3072$.

The structure of such random networks has some important properties, which can be derived with rigorous mathematics for networks whose size becomes unbounded. The theoretical results apply reasonably well to the sample networks that we construct for our simulations. We shall briefly consider the theory and then present aspects of the structure of two particular random networks used in this study.

Some results from the theory of random graphs: expected size of the largest cluster, and why one cluster will be much larger than any of the others when enough junctions exist

Erdös and Rényi[10] studied the properties of "graphs" (networks) with randomly distributed "branches" (junctions) between the "nodes" (cells). In particular, they studied a class of graphs, in which the number of branches is a constant multiplied by the number of nodes, as the number of nodes becomes unbounded. That is, if n is the number of nodes and N the number of branches, then $N = cn$. (Our parameter j, the mean number of junctions attached to each cell, is equal to $2c$.) Erdös and Rényi were interested in properties of the graph that were valid, with probability approaching 1, as n approached infinity.[10]

The most pertinent result in Erdös and Rényi for our purposes concerns the expected size of the largest cluster in graphs (networks) whose overall size becomes unbounded. This result is of biological interest, because it is synchrony among neurons in the largest cluster which will manifest itself in field potential recordings. Erdös and Rényi showed that the (size of the largest cluster)/n approaches 0, for $n \to \infty$, when $c < 0.5$ ($j < 1.0$); when $c > 0.5$ ($j > 1.0$) (the critical connectivity), then (size of the largest cluster)/n is > 0, as $n \to \infty$. That is, the fractional size of the largest cluster, with respect to the whole network, is finite; this fractional size is given by the function $G(c)$, defined below and graphed in Fig. 3:

$$G(c) = 1 - x(c)/2c,$$

where

$$x(c) = \sum_{k=1}^{\infty} (k^{k-1}/k!) \times (2ce^{-2c})^k.$$

Some sample values are as follows: when $c = 0.5945$ ($j = 1.189$ junctions emerging from each cell, on average), then the largest cluster is about 30% of the network; when $c = 0.693$ ($j = 1.386$ junctions emerging from each cell, on average), then the largest cluster is about 50% of the network.

Although the networks used for simulations are not unbounded in size (of course), and are not strictly random (because of distance and connectivity constraints), Erdös and Rényi's $G(c)$ predicts the size of the largest cluster extremely well.[10] To show this, we constructed 11 different networks, with c taking on values 0.525, 0.55, 0.60, …, 1.0. We then calculated the size S of the largest cluster in the generated network (using the computer), and then calculated the c value such that $G(c) = S$. The two c values agreed to within 4% in each case.

The other critical result from the theory of random graphs that is pertinent is this: there can be at most one cluster whose size is of the same order as the entire system. In other words, in random networks that are sufficiently large, there are either 0 or 1 clusters with finite size (as a fraction of the whole network); all of the other clusters have size which approaches 0, relative to the whole network, as the network size becomes unbounded. (One can sketch a proof of this by supposing that one has two large clusters, of size m_1 and m_2, and then estimating the probability of their being disconnected, which they must be for them to be two separate clusters. Add this probability up for all possible m_1 and m_2, and show that it tends to 0 for large n.) What this result means for our simulations is this: if the connectivity is a bit higher than the critical value of $c = 0.5$ ($j = 1.0$), say $j = 1.05$, then there will be exactly one big cluster, and a number of isolated cells and small clusters.

Let us consider, then, the detailed structure of the two random networks used in simulations to be illustrated later in the paper. First, suppose that $c = 0.8$ ($j = 1.6$ gap junctions on each cell, on average). In our sample network, the largest cluster has 1990 cells. The next largest cluster is only 13 cells. There are 449 cells distributed into pairs, triples, …, a 13-tuple, and the remaining 633 cells are isolated. While the connectivity, averaged over the whole network, is 1.6 junctions on each cell, over the large cluster there is an average of 2.17 junctions on each cell. The mean path length on the large cluster is 17.4 ± 6.4. (The distribution of path lengths for this graph is plotted in Fig. 11D). The large cluster contains three cycles: it is not a tree. Second, suppose that $c = 0.525$ ($j = 1.05$ gap junctions on each cell, on average). The largest cluster now has only 261 cells and the next largest cluster has 71 cells; 1093 cells are isolated. Connectivity on the large cluster is 2.01 junctions on each cell, on average. The large cluster contains a three-cycle. Mean path

length on the large cluster is 20.48 ± 11.0. Notice that the mean path length is longer on this 261-cell cluster than it is on the much larger 1990-cell cluster associated with the previous network—as the connection probability approaches the critical value $c = 0.5$, the large cluster becomes more spread out, stringier, so to speak.

Sources of noise in the system

Spontaneous noise arises in axons, as in previous publications (e.g., Ref. 37). In the distal compartment of each axon, there is an independent Poisson process with mean interval Λ, determining whether a current pulse of 0.2 nA, 0.3125 ms is to be applied. Such a current pulse will evoke a spike, unless the cell body is too hyperpolarized (see Results). The spike propagates antidromically, possibly also across gap junction(s), and can evoke excitatory postsynaptic potentials if the latter are being simulated. In different simulations, Λ ranged from 0.5 to 25 s.

Data analysis

The program saved the somatic potential of selected cells, the axon potential (penultimate compartment) of one or two cells, and three average potential signals. Each average signal was of the somatic potentials of 224 pyramidal cells in a 7×32 band of neurons. Fourier transforms were computed of average signals, over 192 ms (1024 data points), after first "apodizing" the waveform (i.e. smoothly attenuating the signal to 0 at the extremes of the time interval). To apodize the signal $w(i)$, we applied the transform $w(i) \rightarrow w(i) \times [\cos(\pi \times (i - 512)/1024)]^2$.

Computing resources

Programs were written in FORTRAN with extra instructions for use on a parallel computer: an IBM 9076 SP2 with 12 nodes. Network simulations were generally run to model 3 s of time, and took about 5 h to run per second. Simulations of small networks (one to three cells) were run on a single node of the computer. Further details can be obtained via e-mail from r.d.traub@bham.ac.uk.

Cellular automaton model

In order to understand better the mathematical properties of our simulated network bursts, we constructed a "model of the model", in which each "neuron" is a cellular automaton with a small number of discrete states, and communication between "neurons" is all-or-none, but with a network topology consisting of a random graph, as for many of the more complex simulations. In this way, we could show that high-frequency oscillations, as simulated here, can be replicated in a model without membrane kinetics. As there are also no synaptic time constants in the cellular automaton model, this approach emphasizes that many features of high-frequency oscillations are determined purely by network structure. Further details of the cellular automaton model are presented in the Appendix.

RESULTS

In the Experimental Procedures, we considered structural aspects of trees and random graphs. Now we shall consider dynamical aspects of neuronal networks, interconnected by axoaxonal gap junctions, where the connection topology consists of a tree or of a random graph. In order to understand the behaviour of large networks, however, it is first necessary to consider properties of two model neurons connected by an axonal gap junction.

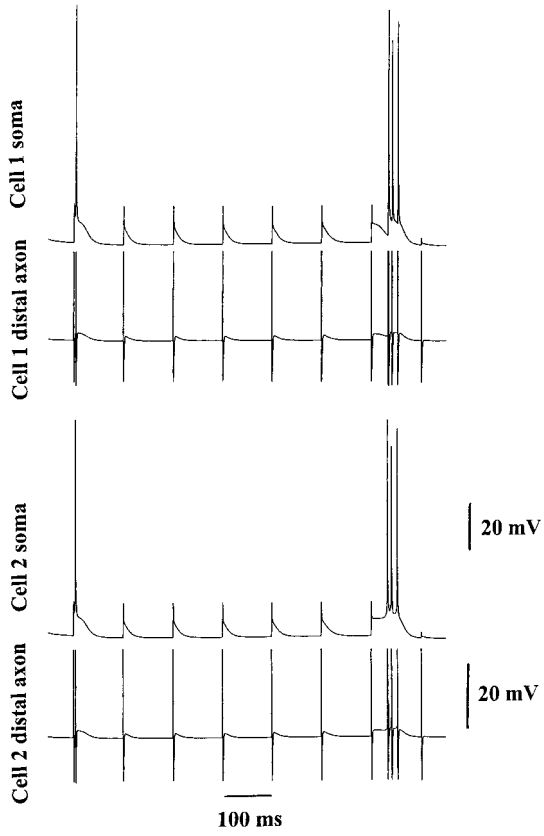

Fig. 4. Behaviour of two model pyramidal cells, coupled by an axoaxonal gap junction, when one of the cells is stimulated antidromically at 10 Hz. Two cells were coupled as shown diagramatically in Fig. 1 (gap junction resistance 273 MΩ). Each cell soma was biased with a 0.2 nA depolarizing current, to shorten the time between network bursts and reduce the length of the simulation. The most distal axon compartment of cell 1 was stimulated "antidromically" by applying 0.2 nA, 0.3125 ms current pulses at 10 Hz. Each of these leads to an axonal spike (shown truncated) that: (a) crosses the gap junction to evoke an axonal spike in cell 2; and (b) invades toward the soma of cell 1. Depending on where the axonal spike blocks, the respective somata respond with: (a) a single action potential with a notch on the upstroke; or (b) a partial spike (about 15 mV amplitude); or (c) a partial spike followed by a burst; or (d) a "spikelet" (amplitude about 3 mV). Note that the single spikes are associated with reflected axonal spikes (see Ref. 41), leading to axonal doublets (intra-doublet interval 4.4 ms). Somatic electrical responses are tightly synchronized between the two cells.

Simulations of pairs of axonally coupled pyramidal cells

Figure 4 illustrates a case where two model pyramidal cells are interconnected (as in Fig. 1) with an axoaxonal gap junction of resistance 273 MΩ, without chemical synaptic interactions. The distal axon of cell 1 is stimulated with brief current pulses (0.2 nA, 0.3125 ms) at 10 Hz, each pulse evoking an action potential. Every axonal spike in cell 1 evokes an axonal spike in cell 2. After an initial burst of action potentials in both neurons (not shown), afterhyperpolarizations (AHPs) develop in each of the neurons. The AHPs

influence the pattern of invasion of the antidromic spikes. Four patterns occur in this figure. (a) A partial spike (~15 mV) followed by a full action potential; note that a reflected spike occurs, detectable as an axon doublet. The intradoublet interval is 4.4 ms, on the long side because of the delay from partial spike to full action potential. (In other instances, e.g., in Fig. 7, antidromic spikes occur that are inflected on the rising phase, but are not preceded by a well-defined partial spike.) (b) Isolated partial spikes (~15 mV). (c) A partial spike followed by a burst. (d) A spikelet (~3 mV). The firing patterns in the two neurons are virtually identical, even though the axon of only neuron 1 was stimulated. Not shown is the behaviour of the IS, but we consistently observed the following: if the distal axon fired an action potential, the spike would reach at least to the axon compartment adjacent to the IS. If, then, the ISs were to fire a full action potential, the soma could respond either with a partial spike or with a full spike, but if the IS responded itself with a partial spike, then a spikelet appeared at the soma.

Figure 5 shows two additional features of the axoaxonal gap junctions used in our simulations. Figure 5A illustrates, on an expanded time scale, a detail of the simulation in Fig. 4: distal axon spikes from each neuron. The peak-to-peak latency is 0.3 ms. Inspection of the data for action potentials in the penultimate axonal compartment—the site of the gap junction—reveals a peak-to-peak latency of 0.25 ms (not illustrated), the minimum time in our model for crossing from one axon to another (for this particular gap junctional resistance). It is interesting that MacVicar and Dudek[17] observed fast prepotentials in some dentate granule cells, after antidromic stimulation of mossy fibres: the latency from action potentials in spike-firing cells to a fast prepotential-firing cell was about 0.2 ms. Perhaps this latency arises from the spread of action potentials between mossy fibres, across gap junctions.

Figure 5B demonstrates that sufficient hyperpolarization of the soma (−14 mV, induced by a −0.3 nA somatic current injection) can prevent distal axonal current pulses from inducing spikes in the model. This observation is important in understanding the lack of spikelets following network bursts.

The simulation of Fig. 4 was repeated using higher frequencies of axonal current pulses delivered to cell 1. When the current pulses occurred at 250 Hz, for example (not illustrated), the axon responded with a full action potential in response to each current pulse, and this action potential faithfully crossed the gap junction to induce firing in the axon of cell 2; the somata responded with 250 Hz partial spikes, tightly synchronized between cells. In addition, each cell might occasionally fire an isolated full action potential, but the full somatic spikes occurred independently in the two cells. Reflected spikes were generated by the somatic action potentials, leading to axonal spike doublets, but the second spike in the axonal doublet was not

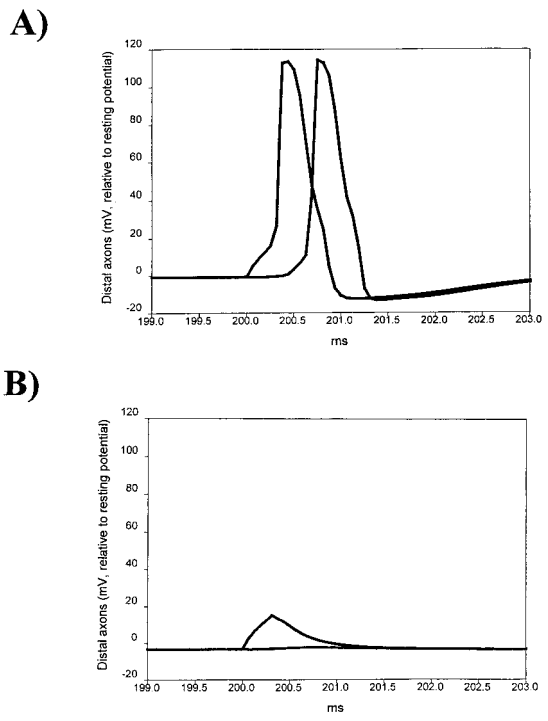

Fig. 5. Latency associated with the axonal gap junction, and regulation of ectopic activity by somatic potential. Two model pyramidal cells were coupled as in Fig. 1, with gap junctional resistance 273 MΩ. Antidromic stimuli (10 Hz) were applied to the distal axon of cell 1, as in Fig. 4, using current pulses to the most distal axonal compartment. Shown are superimposed voltage traces of the most distal axonal compartments of the two cells. (A) When the respective somata are injected with 0.2 nA depolarizing currents, as in Fig. 4, there is a 0.31 ms peak-to-peak latency from the spike in the distal axon of cell 1 to the distal axon of cell 2. Inspection of the potentials at the penultimate axonal compartment, where the gap junction is located (not shown) shows that the peak-to-peak latency across the junction is 0.25 ms. (B) The simulation of A was repeated, but with 0.3 nA hyperpolarizing currents injected into the soma of each cell. This hyperpolarizes the somata by 14 mV and produces 2.6 mV relative hyperpolarization of the distal axon, compared with A. The axonal current pulse no longer induces an action potential in the axon of cell 1.

able to induce firing in the coupled axon. On the other hand (Fig. 6), when current pulses occurred at 400 Hz in the distal axonal compartment of cell 1, then the system's behaviour was different in two respects. First, the axon responded with a full spike only to alternate current pulses, so that it fired at 200 Hz. Each axonal spike in cell 1 induced an axonal spike in cell 2, so that both somata responded (for the most part) with synchronized partial spikes at 200 Hz. Second, somata of the two cells occasionally fired spike multiplets that temporally overlapped, although the spikes were not precisely synchronized on a submillisecond time scale. Clearly, if there are simultaneous multiplets, then the two cells must be co-operating with each other, but as there are no chemical synapses, the question is how this co-operation is possible. Figure 7 shows that the combination of reflected spikes and

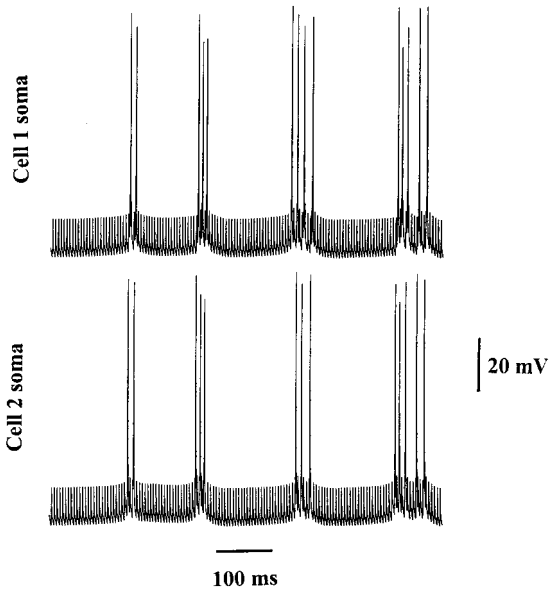

Fig. 6. Co-operative behaviour between two axoaxonally coupled neurons when only one of them is stimulated antidromically at high frequency. The simulation of Fig. 4 was repeated, but with 400 Hz antidromic stimulation of cell 1, rather than 10 Hz. The axons do not follow such a high stimulus frequency 1:1, but usually at only half the stimulus frequency: most of the time, the two somata exhibit synchronized partial spikes at 200 Hz. On occasions, however, the two cells generate spike multiplets, at about the same time, although not always with precise spike/spike synchrony. As the only external input is antidromic to one cell (with the other cell also being excited antidromically because of the gap junction), and without chemical synapses, it is not immediately apparent how the cells communicate with each other, so that the spike multiplets will be temporally correlated (see Fig. 7 for further details).

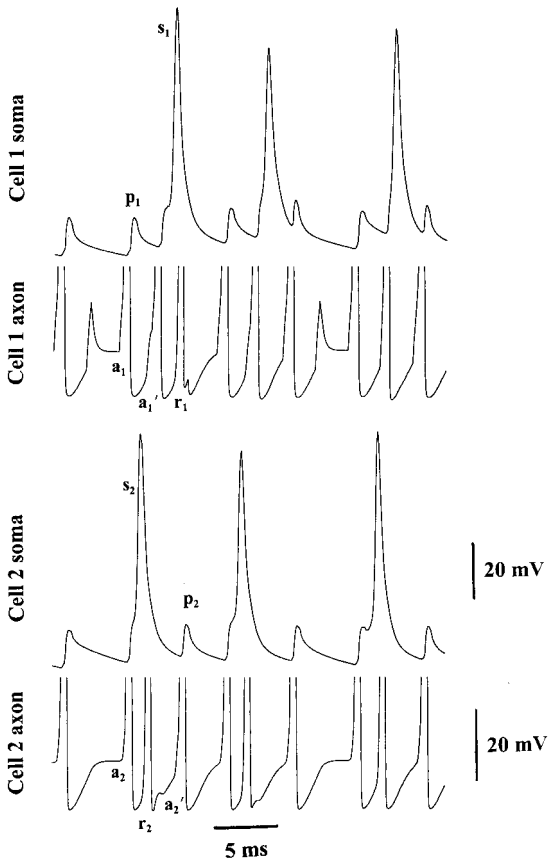

Fig. 7. Co-operative behaviour can arise between antidromically stimulated, axoaxonally connected cells, without chemical synapses, provided the axons are excitable enough, as communication can occur via reflected action potentials. The figure shows data from the simulation of Fig. 6 on an expanded time scale. One example of communication between the neurons will be examined in detail. To explain it, we designate axonal spikes caused by axonal current pulses with "a", reflected axonal spikes with "r", full somatic spikes with "s" and partial somatic spikes with "p", using subscripts 1 or 2, depending on the cell. (The notation used for an axonal spike induced through the gap junction will depend on the origin of the axonal spike on the other side of the junction.) Axonal spike a_1 leads to partial spike p_1, and—crossing the gap junction—to a_2. a_2 induces s_2, causing the reflected spike r_2. This crosses the gap junction to induce a_1': reflected spikes do not, in general, induce spikes across the gap junction, but this particular one arrives just as axon 1 is also being stimulated by a distal current pulse (note that the current pulse alone would also not cause an axonal spike, arriving as it does too soon after a_1). a_1' now causes spike s_1, causing reflected spike r_1 and—crossing the gap junction—a_2' and p_2. The net effect is that the occurrence of an action potential in cell 2, via a reflected spike and aided by the excitation of axon 1, is able to induce an action potential in cell 1.

subthreshold axonal responses to the current pulses allows action potentials in one cell to influence generation of action potentials in the other cell.

Figure 7 consists of a portion of Fig. 6 on an expanded time scale. It allows one to examine the spread of action potentials along axons, across the gap junction, and reflected from the somata. An example of this spread is indicated by the labels a_1 and so forth. To describe the events precisely, let us label the action potentials with letters *a*, *r* and *s*. *a* denotes an axonal spike induced by a current pulse or by spread across the gap junction, *r* denotes an axonal spike induced by reflection from the soma and *s* denotes a somatic spike. *p* shall denote a partial spike in a soma. The subscripts 1 and 2 shall denote soma (or axon) 1 or soma (or axon) 2, respectively. Then, we can trace some of the spread as follows:

$$a_1 \rightarrow p_1$$

$$a_1 \rightarrow a_2 \rightarrow s_2 \rightarrow r_2$$

$$\rightarrow \text{(along with a current pulse) } a_1' \rightarrow s_1 \rightarrow r_1$$

$$\rightarrow a_2' \rightarrow p_2.$$

The essential part about this sequence is this: a full somatic spike in cell 2 has influenced the occurrence of a full somatic spike in cell 1, a few milliseconds later. This happens because the reflected spike from cell 2 is able to induce—across the gap junction—a spike in axon 1. This occurs because the high rate of ectopic current pulses in axon 1 allows the interaction between (i) an ectopic current pulse and (ii) the current induced across the gap junction,

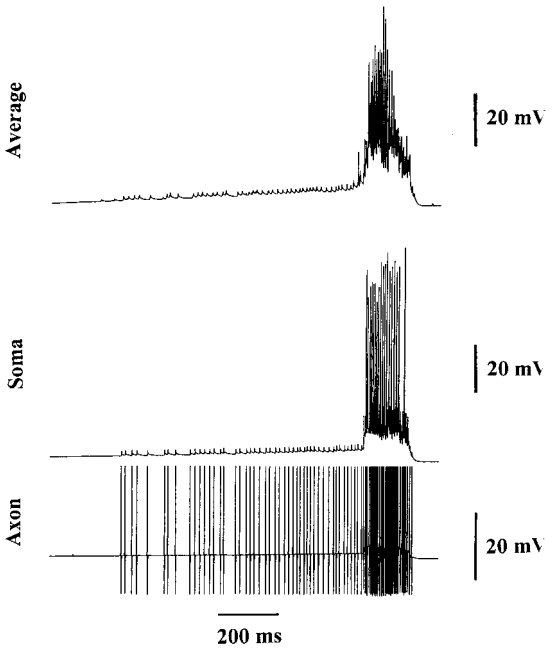

Fig. 8. Synchronized bursting in a network of model pyramidal neurons, interconnected by axoaxonal gap junctions, without chemical synapses. The gap junctional network is a binary tree with 2047 neurons; the remaining 1025 neurons are electrotonically isolated from each other and from the tree. The background rate of axonal current pulses is one per 10 s per axon. The figure shows the average somatic potential of 224 neurons (top), the soma of a single neuron located on the tree (middle) and the axon (at the site of gap junctions) of that same neuron (bottom). A previous network burst had ended about 1 s prior to the beginning of these traces. One can see in the somatic traces the relaxation of the AHP from that previous burst. When the AHP has relaxed enough, spikelets begin to occur, because axonal current pulses become capable of inducing axonal firing (see Fig. 5B). The spikelets are synchronized, as the amplitude is about the same in the average trace as in the single-cell trace, but the synchrony is not precise: spikelets in the average trace do not rise as abruptly as in the single cell, a consequence of the finite time it takes for spikes to propagate across the axonal plexus (Fig. 5A). There is a 1:1 correspondence between spikelets in a given neuron and firing in the axon of that neuron. Note that, once the axon begins firing, it does so at a rate far higher than the rate of current pulses it "sees" at one per 10 s. As somata are not firing prior to the network burst, this shows that axonal spikes are propagating on their own through the axonal plexus (as in Fig. 4). On the other hand, prior to the network burst, not all of the axonal spikes in the system propagate to the axon of the illustrated neuron: if they did, this axon would be firing at an average rate of $2047/10 \simeq 205$ Hz, but the actual frequency (prior to the network burst) is only about 75 Hz. Details of the network burst are shown in Fig. 9. This simulation also shows that network bursting does not require reentry in the axonal plexus: there are no cycles (other than trivial ones) in the tree.

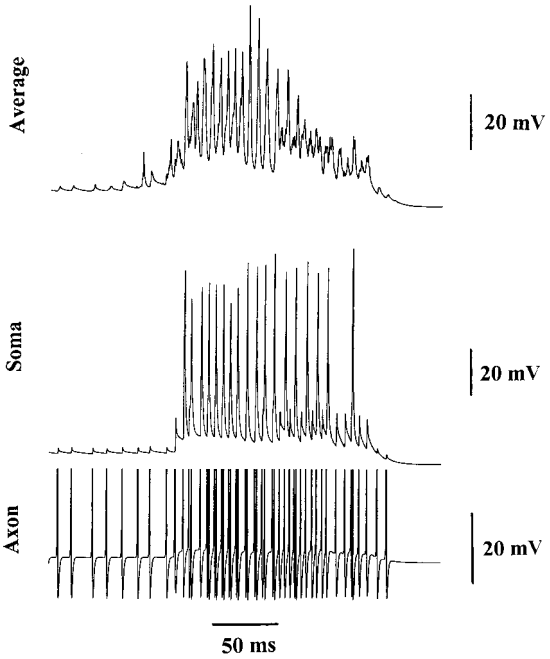

Fig. 9. Axoaxonal gap junctions can produce network bursts exhibiting synchrony on a millisecond time scale. This is the same network burst as in Fig. 8, but on an expanded time scale. The upper trace shows the average somatic potential of 224 pyramidal cells: note the tight synchrony—the 20- to 30-mV amplitude of this average signal indicates that over 25% of the neurons are firing synchronously. Note further that the spikelets preceding the burst are also synchronized, having about the same amplitude as spikelets in individual neurons (middle trace); the synchrony is not perfect, in that the upstroke of the population spikelet is smoother than in a single cell, a consequence of finite propagation times through the electrotonic network. Other features of interest in this figure: neurons exhibit partial spikes and action potentials that are inflected on the upstroke; the axon (below) exhibits—during periods when the soma is firing—spike doublets, representing reflected spikes. The power spectrum of the average signal (upper trace) exhibited peaks at 140 and 172 Hz.

by the reflected spike—recall that, in general, reflected spikes do not cross the gap junction, because of relative refractoriness following the axonal action potential. The further implication of this result is that, in a large network in which there is high-frequency activity percolating through the axonal plexus, there can be opportunities for the firing of some pyramidal cells to influence the firing of other pyramidal cells.

Simulations of networks of axonally coupled pyramidal cells

In this section, we show that simulated networks of axonally coupled pyramidal cells, without chemical synapses, can generate network bursts that are synchronized on a millisecond time scale. Reentrant loops are not required. The network activity is characterized by spikelets and partial spikes, as well as by full action potentials, in cell somata.

Figures 8 and 9 illustrate, on different time scales, the same network burst. The spectral peaks of this event (as measured in the average signal) are at 140 and 172 Hz, so that it is at "high frequency", in the range of high-frequency bursts in the hippocampus. The simulation was performed in the 3072 pyramidal cell network, with a "tree" of axoaxonal gap junctions involving 2047 of the cells (see

Experimental Procedures). As the tree contains no cycles, we can conclude that re-entrant activity through the axonal plexus is not required for the network burst to occur, and that cycles do not play a critical role in determining the oscillation frequency.

The traces in Figs 8 and 9 are: the average somatic potential of 224 pyramidal cells (top), the somatic potential of a cell on the tree (middle trace; cells not on the tree fire only rare isolated single spikes) and the penultimate axonal compartment of the same cell (lower trace, action potentials truncated). The rate of "background" ectopic axonal current pulses was only one per 10 s per axon (0.1 Hz); this, however, implies that, throughout the tree, ectopic current pulses are being delivered at an average of 204.7 Hz. Some detailed features of this simulation are as follows.

1. As the AHPs from the previous network burst (not shown) relax toward resting potential, axonal spikes begin to occur (cf. Fig. 5B).
2. There is a 1:1 correspondence between axon spikes and spikelets in the same neuron, prior to the network burst.
3. Axon spikes, prior to the network burst, are occurring at about 75 Hz. This is about 750 times the ectopic rate in the single axon. The high rate of axonal spikes prior to the network burst cannot be related to reflected spikes, as somata are not firing. We conclude that action potentials are passing from other axons—through gap junctions—to the axon under observation; indeed, the axon under observation is connected to, at most, four other cells, hence spikes must be propagating from some distance away, through the network. There is thus co-operative behaviour in the network, even prior to the onset of the network burst.
4. On the other hand, not all of the axonal spikes popping up in the system are propagating to the axon under observation. If this were true, the firing rate would be closer to 200 Hz. Some of the axonal spikes are being "lost". While we have not documented this phenomenon directly in a large network, loss of spikes will occur via the following mechanisms: (i) if any one axon is bombarded with pulses too fast, there is a limit to how fast it can respond (see above); (ii) if a given axon is approached simultaneously with two action potentials, over two gap junctions on the same compartment, it can fire at most once in response. While this firing may be propagated antidromically to the soma, the firing cannot (because of collision) propagate back across the gap junctions. There are thus annihilations within the network. In summary, only a certain finite amount of action potential "traffic" can propagate through the axonal plexus.
5. There is a 1:1 correspondence between spikelets in the individual cell and spikelets in the average signal: the spikelets are also synchronized. This also demonstrates the propagation of action potentials through the axonal plexus. The upstroke of spikelets in the average signal, however, is not as abrupt as in the single cell, an effect that can be attributed to propagation delays across gap junctions (Fig. 4).
6. Action potentials during the network burst are sometimes inflected on the upstroke (characteristic of antidromic spikes) and are admixed with partial spikes. Axon doublets, a consequence of reflected spikes, are also to be noted. The fact that firing in the different neurons is temporally overlapping can be attributed to two effects: simultaneous relaxation of AHPs in the different cells from the previous burst (but, in general, this is not a stable synchronizing mechanism, as AHPs need not have identical time-courses between cells, and AHPs will be suppressed in low $[Ca^{2+}]_o$ media), and co-operative interactions caused by reflected spikes (Figs 6, 7).

In an attempt to understand how the network burst frequency is determined, we first examined the effects of one parameter: the rate of ectopic axonal current pulses. The simulation of Figs 8 and 9 was repeated with widely different rates of ectopic axonal current pulses: one per 500 ms per axon (2 Hz per axon, 4.094 kHz on the tree as a whole; Fig. 10, upper traces) and one per 20 s per axon (0.05 Hz per axon, 102 Hz on the tree as a whole; Fig. 10, lower traces). Despite the 40-fold difference in the mean rate of ectopic stimulations, the two network bursts in Fig. 10 both have spectral peaks between 100 and 200 Hz. When the ectopic rate is too high, the limited "bandwidth" of the electrotonic network prevents all of the axonal spikes from stimulating any one neuron. On the other hand, when the ectopic rate is low enough, reflected spikes can, in principle, contribute at least some extra spikes to the axonal plexus. (In the cellular automaton model, in contrast, where reflected spikes are not present, oscillation frequency drops progressively as the rate of background "ectopic" events diminishes—see Appendix.)

How then might the frequency of network bursts be determined, if the frequency is so independent of ectopic spike rate (over a large range)? Consider a simple hypothetical situation, of two neurons with an axonal gap junction that contains a "delay line". Suppose the delay line introduces a latency Λ ms for a spike in axon 1 to cross to axon 2. Then, antidromic spikes in cell 1 would be followed Λ ms later by antidromic spikes in cell 2, and vice versa: a characteristic frequency of $1/\Lambda$ has been introduced into the system. In a large network, one expects the characteristic frequency to depend on the average delay between a spike in one axon and a spike in a randomly chosen second axon; this

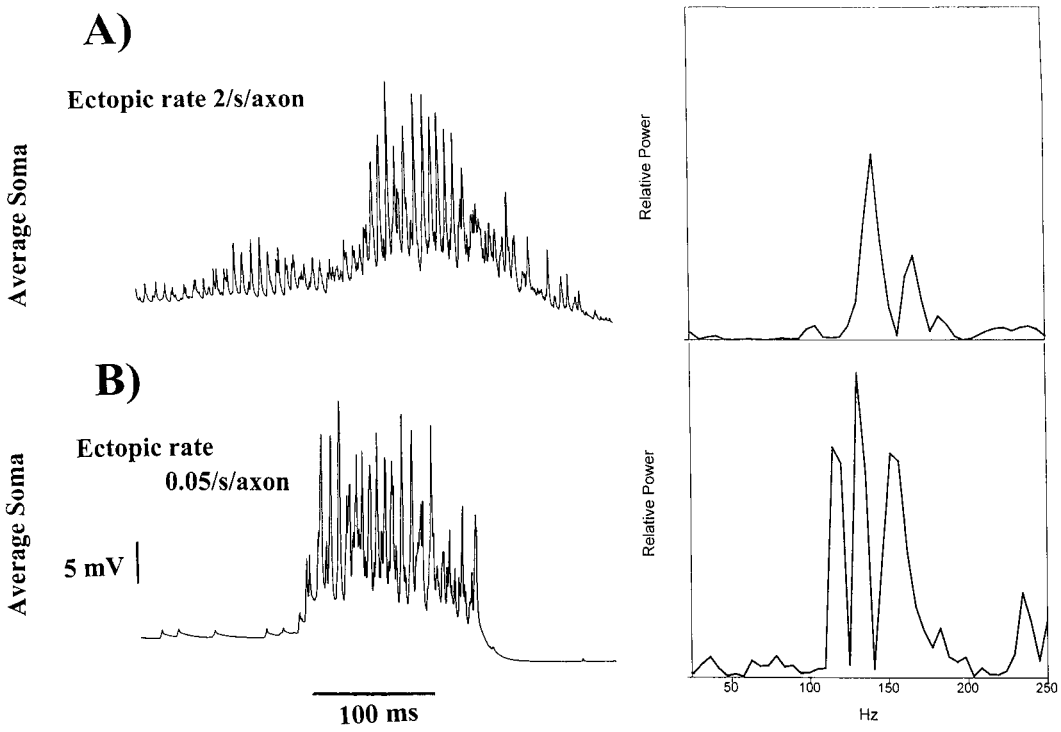

Fig. 10. Network bursts shaped by axoaxonal gap junctions have a similar structure over a 40-fold range of ectopic current-pulse frequency. The simulation of Figs 8 and 9 was repeated for different average frequencies of current pulses delivered to distal axons. In the upper simulation here (average of 224 somatic potentials on the left, power spectrum of this signal on the right), the ectopic pulse rate was one per 0.5 s per axon, or 4094 per second over the connected tree of 2047 cells. In the lower simulation, the ectopic pulse rate was 40 times lower: one per 20 s per axon, or 102 per second over the connected tree. In each case, spectral peaks are between 100 and 200 Hz, and include a peak at about 150 Hz. Evidently, the frequency of the network burst is not determined by the ectopic rate in any simple way: if the ectopic rate is high enough, the network acts as a filter to reduce antidromic stimulation to the neurons (because of limited frequency responses of the axons, and because of contention at branch points), while if the ectopic rate is low enough, the neurons contribute additional activity, probably via reflected spikes.

average delay will be $\Pi \times \Lambda$, where Π is the mean path length in the network. In the tree (see Experimental Procedures), the mean path length is about 16 and the latency to cross a gap junction (resistance 273 MΩ) is about 0.25 ms, under baseline conditions in two-cell networks (perhaps more than this in large networks, where multiple gap junctions increase the impedance load). We estimate that the oscillation frequency would then be at most $1/(16 \times 0.25)$ kHz, or about 250 Hz, a figure somewhat higher than that which is usually observed.

A prediction of the above argument is that a decrease in latency, for spikes to cross the axoaxonal gap junction, should cause an increase in oscillation frequency. This prediction was confirmed in the simulation of Fig. 11A and B: the simulation of Fig. 10 (upper traces) was repeated, but with gap junction resistance of 191 MΩ, instead of the previous 272 MΩ (in two-cell networks, this reduction in gap junction resistance reduces the latency for a spike crossing the junction from about 0.25 ms to about 0.19 ms). The resulting network burst (Fig. 11A) is faster than in Fig. 10 (upper trace), having a spectral peak of 182 Hz, compared with the previous peak at 144 Hz. Indeed, the frequency change is about that predicted by the formula: oscillation interval $= \Pi \times \Lambda$; this formula predicts that the ratio of oscillation frequencies will be the inverse of the ratio of gap junction latencies: note that 182 Hz/144 Hz = 1.26, while 0.25 ms/0.19 ms = 1.32.

One interesting feature of a large binary tree is that the distribution of path lengths between pairs of cells is relatively narrow (Fig. 11C). This would be expected to contribute to the synchrony of the population firing. In contrast, in the large cluster of a random graph (average 1.6 junctions on each cell), the distribution of path lengths is relatively broadened (Fig. 11D). One might guess that population bursts, in which the electrotonic network is a random graph, would be less synchronized than on a tree.

The next question to be addressed, therefore, was whether high-frequency synchronized network bursts could be generated in random axoaxonally coupled neuronal networks, and—if so—how synchronized they would be. The simulation of Fig. 12 demonstrates that network bursts can be generated in randomly connected networks, but, as expected, synchronization can be reduced relative to

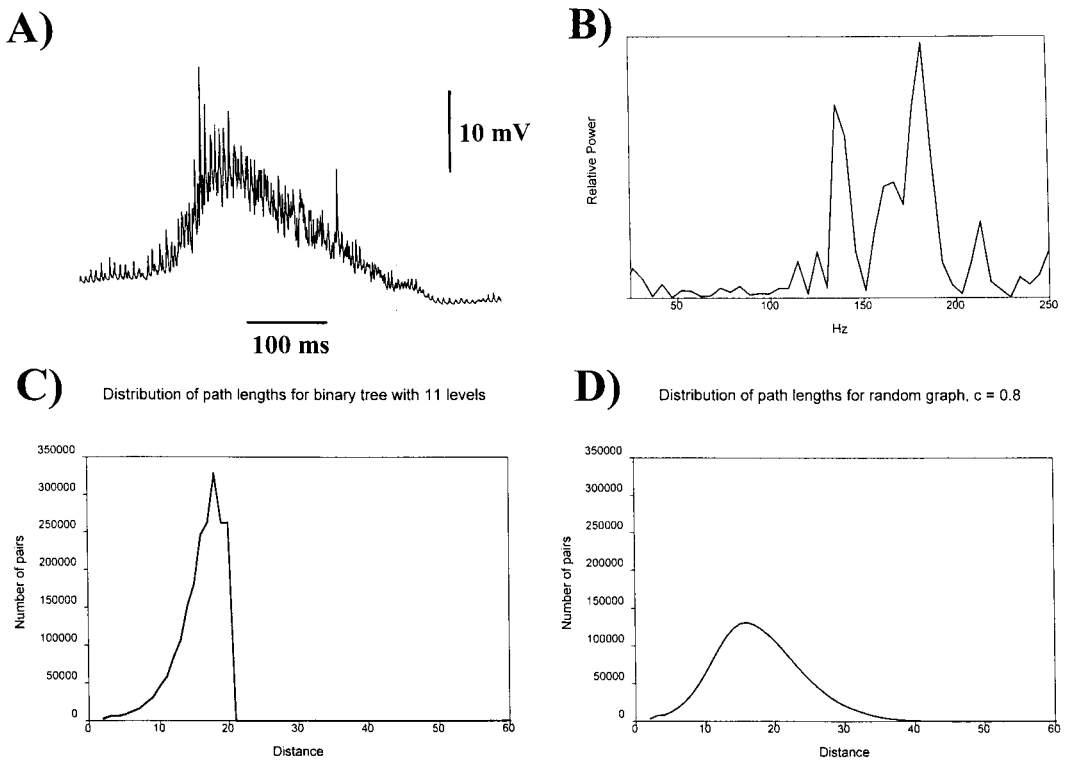

Fig. 11. Increasing axoaxonal gap junctional conductance raises the frequency of network bursts; path lengths in a tree are narrowly distributed, but are broadly distributed in a random network. (A) The simulation of Fig. 10 (upper traces) was repeated, using the tree electrotonic network, and an ectopic current pulse rate of one per 0.5 s per axon, but in the present case, gap junction resistance was reduced from the usual 273 MΩ to 191 MΩ (conductance 5.2 nS). The resulting network burst is faster than in Fig. 10 (power spectrum in B, peak at 182 Hz, vs peak at 144 Hz for the upper trace of Fig. 10). (C) The distribution of path lengths in the 2047-neuron binary tree used in the above simulations. This distribution is relatively narrow, a feature that contributes to the synchrony of the network bursts. (D) The distribution of path lengths in the large cluster (1990 cells) of a random network (each cell having, on average, 1.6 gap junctions). This distribution is broad, and might be expected to reduce the synchrony of network bursts (see below).

the synchrony observed in a tree of size comparable to the size of the large cluster in the random network.

The network used to generate the burst in Fig. 12 was random, with an average of 1.6 gap junctions on each axon, and with 1990 cells in the large cluster (see Experimental Procedures): this is the network whose large-cluster path length distribution is shown in Fig. 11D. The spectral peak of the average signal (uppermost trace of Fig. 12) was 141 Hz. While the synchronized spikelets preceding the burst (about 2 mV in amplitude in the average signal), and the form of the burst itself, somewhat resemble the event of Figs 8 and 9, there are certain important differences:

1. The build-up of spikelets prior to the network burst is not as rhythmic as in the tree (Figs 8 and 9).
2. The amplitude of the network burst is only about 20% of the amplitude generated by the tree, although the large cluster here is 1990/2047 = 97% of the size of the tree. The reason for this is, as Fig. 12 demonstrates, that not all of the neurons in the large cluster fire coincident with the network burst; indeed, we found one neuron on the large cluster that rarely fired at all, just like cells on small clusters (one of the latter is illustrated at the bottom of Fig. 12).
3. The duration of the network burst is somewhat shorter than in Figs 8 and 9, although the rate of ectopic current pulses used in Fig. 12 was 2 Hz per axon (3980 Hz over the whole large cluster).

We suspect that the reduced synchrony of the random network relative to the tree is related to the distribution of path lengths in the random graph. While the mean path length, in the large cluster of the random graph used for Fig. 12, is 17.7 ± 6.4 (compared with 16.0 ± 3.3 for the tree, not so different), the maximum path length in the large random cluster is 53, compared with only 20 on the tree. The fact that the large cluster in the random network is, so to speak, more spread out than in the tree, may increase the chances that axonal spikes are blocked as they "try" to percolate through the axonal plexus; such blocking would, in turn, reduce the synchronization. In addition, there will be a broad distribution of times that it takes for an

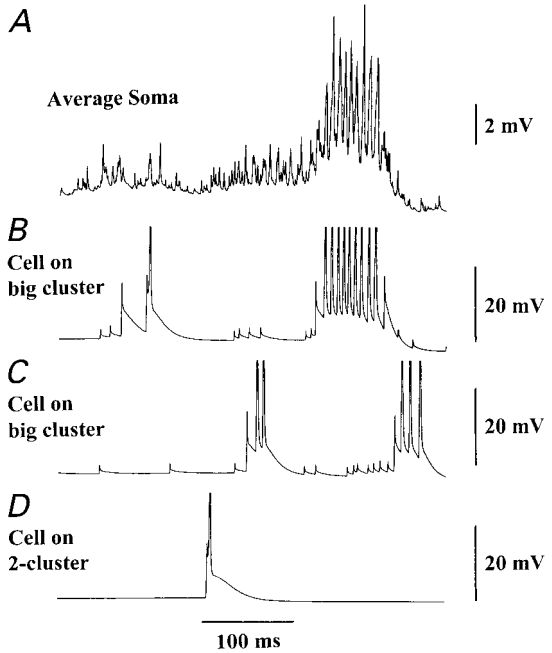

Fig. 12. A network burst generated by a randomly connected network of axoaxonally coupled neurons may be less synchronized than a burst generated on a tree of similar size, average connectivity and average path length. This figure illustrates a network burst generated in the 3072-cell system when there are an average of 1.6 gap junctions/neuron, placed randomly, with a background ectopic pulse rate of two per second per axon. In this example, the large cluster has 1990 cells, with an average path length of 17.7 ± 6.4, maximum path length 53 and an average of 2.17 junctions per neuron on the big cluster. For comparison, the tree used in the simulation of Figs 8 and 9 had 2047 neurons, average path length 16.0 ± 3.3, maximum path length 20, average 2.00 junctions per neuron on the tree. (A) The average somatic potential of 224 cells. (B, C) Somatic potential of two neurons on the big cluster. (D) Somatic potential of a neuron that is not on the big cluster and is electrotonically connected, axoaxonally, to one other neuron only. (Action potentials are truncated). Note that the amplitude of the average signal is about one-fifth the amplitude of the average signal in Fig. 10, a result of the fact that bursting of neurons on the big cluster does not always occur in the same time window (B, C). Cells not on the big cluster do not burst (D) and fire only rarely. As before, there are also spikelets and partial spikes. The reduced synchrony of this burst compared to the burst generated on the tree, despite similar size of the large cluster and similar mean junctions/neuron and path lengths, may be a result of the greater spread of path lengths in the random network.

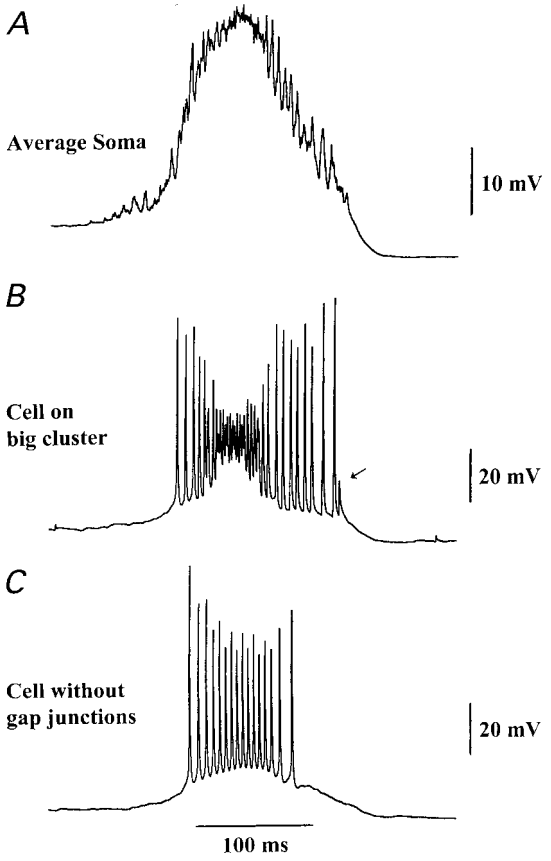

Fig. 13. A random axoaxonal electrotonic network, in combination with a random recurrent excitatory synaptic network, can lead to "population spikes" superimposed on the epileptiform synchronized burst. This figure illustrates a network burst amongst pyramidal cells that is shaped both by axoaxonal gap junctions (network parameters as in Fig. 12), together with a random network of recurrent excitatory synapses (30 presynaptic cells per neuron, location of connections on basal dendrites, unitary EPSC 0.25 $te^{-t/2}$ nS, t in ms). (A) Average somatic potential of 224 pyramidal cells. (B) Soma of a pyramidal neuron that is on the large cluster of the electrotonic network. (C) Soma of a neuron that is electrotonically isolated. (Of course, with 30 inputs per cell, all neurons lie in the synaptic network.) The average signal (A) shows a large slow depolarization mediated by excitatory synaptic currents and g_{Ca}, superimposed on which is a fast oscillation (182 Hz), resembling population spikes occurring during an epileptiform field potential in the hippocampus.[25] There are fewer spikelets than when synaptic conductances are absent: note that ectopic axonal activity now leads to induction of excitatory postsynaptic potentials, as well as antidromic activity, and this background of synaptic activity may mask the spikelets. A partial spike is noted in the cell on the large cluster (B), but not in the isolated cell (C). Cells on the large cluster were consistently more depolarized than were electrotonically isolated cells, because the former neurons could be excited both synaptically and by barrages of antidromic spikes.

ectopic spike to percolate through the network, an effect which might "smear out" the population spikes.

Simulations of networks of pyramidal neurons, interconnected by axoaxonal gap junctions, as well as by recurrent excitatory synapses

The simulation of Fig. 13 demonstrates that axoaxonal gap junctions and recurrent excitatory synapses can work together, shaping a network burst with a slow depolarizing component, along with a high-frequency, population spike-resembling component, 182 Hz in the example illustrated. For this simulation, the electrotonic network was the random network used for the simulation of Fig. 12 (average of 1.6 gap junctions on each axon, 1990 cells in the large cluster). The background rate of ectopic axonal current pulses was, on average, 2 Hz per axon. The synaptic network, as described in the Experimental Procedures, has 30 presynaptic cells per neuron (and hence is topologically connected:

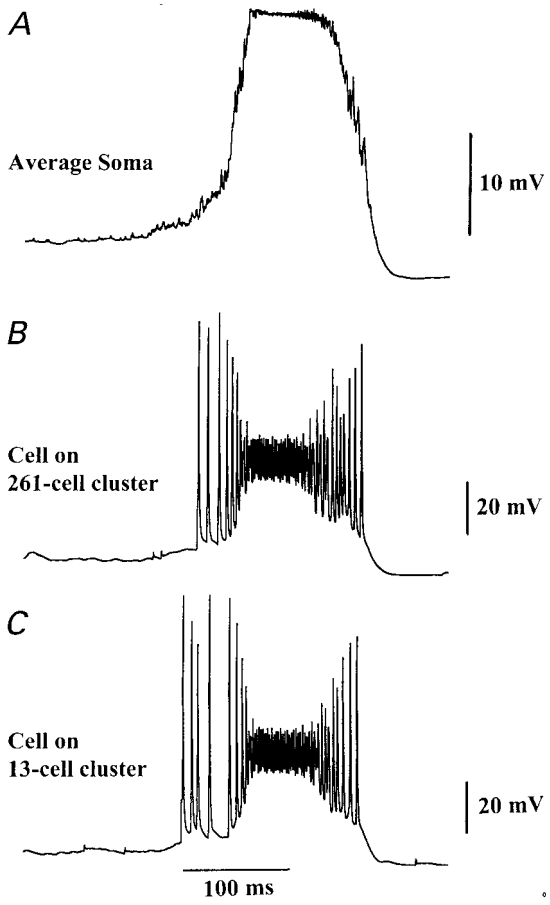

Fig. 14. "Population spikes" are attenuated when there are too few axoaxonal gap junctions. The simulation of Fig. 13 was repeated with two alterations: (a) the electrotonic network was random but with an average density of only 1.05 junctions per neuron; (b) unitary EPSCs were doubled in amplitude (leaving them the same amplitude meant that synchronized bursts would not occur). Parameters of the electrotonic network included: the large cluster had 261 cells, with mean path length 20.5 ± 11.0 and maximum path length 52; average 2.01 junctions per neuron on the large cluster. (A) Average somatic potential of 224 neurons, showing the large slow depolarization during a network burst, but with attenuated synchronized high-frequency activity. (B) Somatic potential of a cell on the large cluster, showing spikelets but no partial spikes. (C) Somatic potential of a cell on an electrotonic 13-cluster, again showing spikelets but no partial spikes. Indeed, the firing pattern is quite similar to that of the cell on the large cluster.

there are no isolated cells). The figure shows an average signal (top: 224 pyramidal cell somatic potentials), the somatic potential of a neuron on the large cluster of the electrotonic network (middle trace) and a neuron that is electrotonically isolated (lower trace). Besides the existence of "population spikes", the figure shows that the firing patterns of neurons on the large cluster are different from those for neurons that are isolated (this was consistently the case, not just for the examples shown): neurons on the large electrotonic cluster become more depolarized and have longer bursts; in addition, cells on the large cluster sometimes generated partial spikes (see the last spike in the middle trace). These features presumably result because such neurons are bombarded both by synaptic excitation[15,45] and by antidromic spikes, while electrotonically isolated cells are excited only synaptically.

We next asked whether the "population spikes" in Fig. 13 depended on the size of the large cluster in the electrotonic network. The simulation of Fig. 13 was therefore repeated using a more sparse electrotonic network, a random network with an average of only 1.05 gap junctions on each axon, with a large cluster size of only 261 cells (see Experimental Procedures). In this case, synchronous bursts did not occur (not shown): in order to obtain synchronous bursts, it was necessary to increase the amplitude of unitary excitatory postsynaptic currents (EPSCs), demonstrating that a sufficient density of axoaxonal gap junctions can lower the threshold for generating epileptiform synchronized bursts, in simulations. When unitary EPSCs were twice as large as in Fig. 13, but with an electrotonic network having only 1.05 gap junctions on each axon on average, the network burst shown in Fig. 14 resulted. Note that the "population spikes" are now severely attenuated. An experimental prediction suggested by this result is the following: axoaxonal gap junctions could, in principle, contribute to the high-frequency component of the epileptiform field potential, in addition to (or perhaps instead of) ephaptic interactions.

DISCUSSION

Our simulations demonstrate that, in principle, networks of randomly interconnected pyramidal neurons, joined by axoaxonal gap junctions, can generate 100–200 Hz synchronized oscillations either (i) in the absence of synaptic transmission or (ii) in combination with recurrent excitatory synaptic connections. The oscillations so generated are transient, a consequence of intrinsic cellular AHPs. Simulated somatic potentials include antidromic action potentials, rising abruptly and sometimes having inflections on the rising phase, spikelets (rapidly rising depolarizing potentials of up to 5 mV) and partial spikes (action potential-like transients, 10–20 mV in amplitude). All of these potentials, in simulations, are somatic responses to axonal spikes.

The important elements in our model are these:

1. A collection of gap junctions between axons, with the property that an action potential in one axon can induce an action potential in a connected axon.
2. A background of spontaneous current pulses to the axons, which are capable of inducing action potentials, provided the soma is not too hyperpolarized. If spontaneous axonal spikes were to originate much further from the soma than was assumed in our model, then the soma potential

would presumably become irrelevant for this induction.
3. The variable responses to antidromic spikes of cell somata, depending upon invasion of the IS and upon somatic membrane potential: spikelet, partial spike or full action potential (or, occasionally, a burst, as can also happen experimentally when synaptic inhibition is suppressed[41]).
4. Reflected spikes from the cell soma: also a phenomenon that has been demonstrated experimentally.[41]

The signals generated by the model, both cell averages (which correspond approximately to field potentials) and intracellular potentials, resemble experimental recordings,[7,25,42] particularly those obtained in low-Ca^{2+} media, although we did not block g_{Ca} and Ca^{2+}-dependent currents in the model neurons. The high-frequency population oscillations so generated could account for the high-frequency component of epileptiform field potentials (Fig. 13), and possibly also for *in vivo* ripples.[52]

The physical principles governing the structure of the network bursts appear simple: in essence, a source of background spikes and strong coupling between axons (also see Appendix; "strong" here refers not to the conductance value of the gap junction *per se*, but rather to the ability of action potentials to propagate across the junction). The origin of the oscillation frequency is, however, much more subtle, depending as it appears to on a topological property of the network: the mean path length between cells. This dependence of frequency on signal delay is reminiscent of the dependence of frequency on signal delays around a network loop, in re-entrant rhythms, such as occur in certain of the tachycardias (e.g., Wolff–Parkinson–White syndrome). The physically interesting distinction is that, in model hippocampal networks with axoaxonal coupling, the relevant signal delay is not around a loop—indeed, oscillations can occur when the network contains no loops; instead, the delay is in propagation from cells to other cells. This oscillation mechanism is also to be distinguished from mechanisms in which (i) the population frequency is determined by the frequency at which soma/dendritic membranes will fire (or burst) when depolarized (example: secondary bursts in a seizure discharge, which occur when slow synaptic currents induce dendritic bursting[43]); and from (ii) oscillations in which frequency is determined primarily by a synaptic time constant (example: gamma frequency oscillations in pharmacologically isolated networks of interneurons[44]).

In relating the simulations to experimental observations, there are several considerations.

1. As discussed in association with Fig. 11, the frequency of the network oscillation should vary inversely with the latency of spread of action potentials through the axonal plexus. Interestingly, halothane (a gap junction blocker) lowers the frequency (by as much as 50%) of network oscillations in the medullary pacemaker nucleus of a weakly electric fish, a nucleus in which the cells are interconnected only by gap junctions.[19]
2. So far as we are aware, there is no direct morphological evidence that pyramidal cell axoaxonal gap junctions actually exist in the hippocampus. Such gap junctions do exist in other systems, such as the medullary pacemaker nucleus of weakly electric fish,[9,36] and the physiological evidence (spikelets and partial spikes, shape of network bursts) and pharmacological evidence (sensitivity of high-frequency bursts to treatments that reduce or augment gap junctional conductances) are both consistent with the existence of axoaxonal gap junctions.[7] Nevertheless, there is no substitute for anatomical observation. Anatomy should also indicate where on axons the putative gap junctions are located, a parameter which will have physiological relevance.
3. Assuming that axoaxonal gap junctions are proven to exist in the hippocampus, what is their average density and spatial pattern? If the spatial pattern can be assumed random, and the density of gap junctions uniform and above the critical value of $j = 1$ (i.e. each axon has, on average, at least one gap junction), then Erdös and Rényi,[10] or simulations, allow one to make predictions on the size of the large cluster, and on the distribution of sizes for small clusters. These numbers, in turn, allow one to predict the fraction of cells which participate in network bursts—a number that may be experimentally measurable. Our data imply the remarkable conclusion that high-frequency network oscillations can occur when axoaxonal gap junctions are sparse: less than two junctions, on average, on each axon.
4. Assuming that axoaxonal gap junctions exist in the hippocampus, how might they be regulated by active currents[5] and by neuromodulators?[22]
5. Assuming that axoaxonal gap junctions exist in the hippocampus, what might be the functional implications? This is a knotty question, which has two components: (i) what is the function (if any) of synchronized high-frequency oscillations in the mammalian brain? (ii) What would be the consequences of generating high-frequency oscillations by axoaxonal gap junctions, as opposed to some other mechanism?

As far as question (i) is concerned: the fish medullary pacemaker nucleus is a "central pattern generator" of clear function. The frequency of network oscillation in this nucleus is the frequency at which the fish generates an alternating electric current. The cells in the nucleus need to oscillate synchronously so that different portions of the electric organ will not produce currents that cancel each other in the water surrounding the fish. On the other

hand, hippocampal pyramidal cells, so far as we are aware, are not connected to other neurons where a 100–200 Hz signal—and a transient one, at that—have functional meaning. We therefore regard the function—if any—of the high-frequency oscillation as unknown.

Concerning question (ii): it is possible that axo-axonal gap junctions are present in order to define assemblies of pyramidal cells.[50] Pyramidal cells so linked would be coupled with a speed and security that cannot be obtained with recurrent synaptic excitation.[6,18] The reason is that axoaxonal gap junctions can, in principle, allow reliable transmission of action potentials with submillisecond latency (Fig. 5). Suppose, for example, that pyramidal cells P_1, P_2, …, P_n are axoaxonally coupled, either directly or indirectly, with mean path length Π, and spike latency across a junction Λ (~ 0.25 ms). If Q is a neuron postsynaptic to any of the P_i (say P_1), and any of the P_i fire, then Q will be excited—the difference in latency that this excitation has, from the normal $P_1 \rightarrow Q$ latency, will have an expected value of $\Pi \times \Lambda$ ms. In general, Q will be excited multiply, by some subset (or all) of the P_i. The cells P_1, …, P_n have, so to speak, lost their individuality and become a unit.

Of course, if this arrangement were common in the brain, one would expect to see frequent manifestations of antidromic activation of neurons: partial spikes, antidromic spikes, and so forth. Axoaxonic interneurons, generating inhibitory postsynaptic potentials on axon ISs[2,28] may serve to suppress some of this antidromic activation.

Ephaptic interactions vs gap junctions in synchronizing action potentials during high-frequency oscillations

Our data do not have implications—either positive or negative—for a role of ephaptic interactions in providing synchrony of high-frequency activity.[14,27,33] The data imply, rather, that gap junctions could also play a role. We do suspect, however, that ephaptic interactions play little part in the spontaneous high-frequency oscillations described by Draguhn *et al.*,[7] given the small amplitude of the field potentials (tens of microvolts) and the estimates of 5 mV/mm of extracellular potential gradients that are required to influence neuronal activity.[13]

CONCLUSION

Network simulations suggest that axon/axon gap junctions, sparsely and randomly distributed amongst pyramidal cells, could account for high-frequency neuronal population oscillations, without a necessary participation of chemical synapses.

Acknowledgements—We thank L. S. Schulman, T. J. Sejnowski, K. T. Moortgat, C. M. Anderson, R. Empson and G. Buzsáki for helpful discussions, A. Bibbig for reading over the manuscript, and P. Mayes and W. Weir for important help with the parallel computer. This work was supported by the Wellcome Trust, Human Frontier and the DFG. R.D.T. is a Wellcome Principal Research Fellow.

REFERENCES

1. Bennett M. V. L. (1977) Electrical transmission: a functional analysis and comparison to chemical transmission. In *Handbook of Physiology*, Section 1: *The Nervous System*, Vol. 1: *Cellular Biology of Neurons*, Part 1 (ed. Kandel E. R.), pp. 357–416. American Physiological Society, Bethesda, MD.
2. Buhl E. H., Han Z.-S., Lörinczi Z., Stezhka V. V., Karnup S. V. and Somogyi P. (1994) Physiological properties of anatomically identified axo-axonic cells in the rat hippocampus. *J. Neurophysiol.* **71,** 1289–1307.
3. Buzsáki G., Horváth Z., Urioste R., Hetke J. and Wise K. (1992) High-frequency network oscillation in the hippocampus. *Science* **256,** 1025–1027.
4. Chrobak J. J. and Buzsáki G. (1996) High-frequency oscillations in the output networks of the hippocampal–entorhinal axis of the freely behaving rat. *J. Neurosci.* **16,** 3056–3066.
5. Debanne D., Guérineau N. C., Gähwiler B. H. and Thompson S. M. (1997) Action-potential propagation gated by an axonal I_A-like K^+ conductance in hippocampus. *Nature* **389,** 286–289.
6. Deuchars J. and Thomson A. M. (1996) CA1 pyramid–pyramid connections in rat hippocampus *in vitro*: dual intracellular recordings with biocytin filling. *Neuroscience* **74,** 1009–1018.
7. Draguhn A., Traub R. D., Schmitz D. and Jefferys J. G. R. (1998) Electrical coupling underlies high-frequency oscillations in the hippocampus *in vitro*. *Nature* **394,** 189–192.
8. Dye J. and Heiligenberg W. (1987) Intracellular recording in the medullary pacemaker nucleus of the weakly electric fish, *Apteronotus*, during modulatory behaviors. *J. comp. Physiol. A* **161,** 187–200.
9. Elekes K. and Szabo T. (1985) Synaptology of the medullary command (pacemaker) nucleus of the weakly electric fish (*Apteronotus leptorhynchus*) with particular reference to comparative aspects. *Expl Brain Res.* **60,** 509–520.
10. Erdös P. and Rényi A. (1960) On the evolution of random graphs. *Publ. Math. Inst. Hung. Acad. Sci.* **5,** 17–61.
11. Fisher R. S., Webber W. R. S., Lesser R. P., Arroyo S. and Uematsu S. (1992) High-frequency EEG activity at the start of seizures. *J. clin. Neurophysiol.* **9,** 441–448.
12. Haas H. L. and Jefferys J. G. R. (1984) Low-calcium field burst discharges of CA1 pyramidal neurones in rat hippocampal slices. *J. Physiol.* **354,** 185–201.
13. Jefferys J. G. R. (1981) Influence of electric fields on the excitability of granule cells in guinea-pig hippocampal slices. *J. Physiol.* **319,** 143–152.
14. Jefferys J. G. R. and Haas H. L. (1982) Synchronized bursting of CA1 hippocampal pyramidal cells in the absence of synaptic transmission. *Nature* **300,** 448–450.
15. Johnston D. and Brown T. H. (1981) Giant synaptic potential hypothesis for epileptiform activity. *Science* **211,** 294–297.
16. MacVicar B. A. and Dudek F. E. (1981) Electrotonic coupling between pyramidal cells: a direct demonstration in rat hippocampal slices. *Science* **213,** 782–785.

17. MacVicar B. A. and Dudek F. E. (1982) Electrotonic coupling between granule cells of the rat dentate gyrus: physiological and anatomical evidence. *J. Neurophysiol.* **47,** 579–592.
18. Miles R. and Wong R. K. S. (1986) Excitatory synaptic interactions between CA3 neurones in the guinea-pig hippocampus. *J. Physiol.* **373,** 397–418.
19. Moortgat K. T., Bullock T. H. and Sejnowski T. J. (1998) Blocking gap junctions in the electric fish pacemaker nucleus alters the frequency and synchrony of oscillations. *Soc. Neurosci. Abstr.* **24,** 186.
20. Moortgat K. T., Keller C. H., Bullock T. H. and Sejnowski T. J. (1998) Submicrosecond pacemaker precision is behaviorally modulated: the gymnotiform electromotor pathway. *Proc. natn. Acad. Sci. U.S.A.* **95,** 4684–4689.
21. Patrylo P. R., Kuhn A. J., Schweitzer J. S. and Dudek F. E. (1996) Multiple-unit recordings during slow field-potential shifts in low-$[Ca^{2+}]_o$ solutions in rat hippocampal and cortical slices. *Neuroscience* **74,** 107–118.
22. Perez Velazquez J. L., Han D. and Carlen P. L. (1997) Neurotransmitter modulation of gap junctional communication in the rat hippocampus. *Eur. J. Neurosci.* **9,** 2522–2531.
23. Perez Velazquez J. L., Valiante T. A. and Carlen P. L. (1994) Modulation of gap junctional mechanisms during calcium-free induced field burst activity: a possible role for electrotonic coupling in epileptogenesis. *J. Neurosci.* **14,** 4308–4317.
24. Rash J., Duffy H. S., Dudek F. E., Bilhartz H. L., Whalen L. R. and Yasumura T. (1977) Grid-mapped freeze-fracture analysis of gap juncitons in gray and white matter of adult rat central nervous system, with evidence for a "pan-glial syncytium" that is not coupled to neurons. *J. comp. Neurol.* **388,** 265–292.
25. Schwartzkroin P. A. and Prince D. A. (1977) Penicillin-induced epileptiform activity in the hippocampal *in vitro* preparation. *Ann. Neurol.* **1,** 463–469.
26. Schwartzkroin P. A. and Prince D. A. (1978) Cellular and field potential properties of epileptogenic hippocampal slices. *Brain Res.* **147,** 117–130.
27. Snow R. W. and Dudek F. E. (1984) Electrical fields directly contribute to action potential synchronization during convulsant-induced epileptiform bursts. *Brain Res.* **323,** 114–118.
28. Somogyi P., Freund T. F. and Cowey A. (1982) The axo-axonic interneuron in the cerebral cortex of the rat, cat and monkey. *Neuroscience* **7,** 2577–2607.
29. Spencer W. A. and Kandel E. R. (1961) Electrophysiology of hippocampal neurons. IV. Fast prepotentials. *J. Neurophysiol.* **24,** 272–285.
30. Stasheff S. F., Hines M. and Wilson W. A. (1993) Axon terminal hyperexcitability associated with epileptogenesis *in vitro*. I. Origin of ectopic spikes. *J. Neurophysiol.* **70,** 960–975.
31. Stasheff S. F., Mott D. D. and Wilson W. A. (1993) Axon terminal hyperexcitability associated with epileptogenesis *in vitro*. II. Pharmacological regulation by NMDA and $GABA_A$ receptors. *J. Neurophysiol.* **70,** 976–984.
32. Swann J. W., Brady R. J., Friedman R. J. and Smith E. J. (1986) The dendritic origins of penicillin-induced epileptogenesis in CA3 hippocampal pyramidal cells. *J. Neurophysiol.* **56,** 1718–1738.
33. Taylor C. P. and Dudek F. E. (1982) Synchronous neural afterdischarges in rat hippocampal slices without active chemical synapses. *Science* **218,** 810–812.
34. Taylor C. P. and Dudek F. E. (1984) Excitation of hippocampal pyramidal cells by an electrical field effect. *J. Neurophysiol.* **52,** 126–142.
35. Taylor C. P. and Dudek F. E. (1984) Synchronization without active chemical synapses during hippocampal afterdischarges. *J. Neurophysiol.* **52,** 143–155.
36. Tokunaga A., Akert K., Sandri C. and Bennett M. V. L. (1980) Cell types and synaptic organization of the medullary electromotor nucleus in a constant frequency weakly electric fish, *Sternarchus albifrons*. *J. comp. Neurol.* **192,** 407–426.
37. Traub R. D., Colling S. B. and Jefferys J. G. R. J. (1995) Cellular mechanisms of 4-aminopyridine-induced synchronized after-discharges in the rat hippocampal slice. *J. Physiol.* **489,** 127–140.
38. Traub R. D. and Dingledine R. (1990) Model of synchronized epileptiform bursts induced by high potassium in CA3 region of rat hippocampal slice. Role of spontaneous EPSPs in initiation. *J. Neurophysiol.* **64,** 1009–1018.
39. Traub R. D., Dudek F. E., Snow R. W. and Knowles W. D. (1985) Computer simulations indicate that electrical field effects contribute to the shape of the epileptiform field potential. *Neuroscience* **15,** 947–958.
40. Traub R. D., Dudek F. E., Taylor C. P. and Knowles W. D. (1985) Simulation of hippocampal afterdischarges synchronized by electrical interactions. *Neuroscience* **14,** 1033–1038.
41. Traub R. D., Jefferys J. G. R., Miles R., Whittington M. A. and Tóth K. (1994) A branching dendritic model of a rodent CA3 pyramidal neurone. *J. Physiol.* **481,** 79–95.
42. Traub R. D., Jefferys J. G. R. and Whittington M. A. (1994) Enhanced NMDA conductances can account for epileptiform activities induced by low Mg^{2+} in the rat hippocampal slice. *J. Physiol.* **478,** 379–393.
43. Traub R. D., Miles R. and Jefferys J. G. R. (1993) Synaptic and intrinsic conductances shape picrotoxin-induced synchronized after-discharges in the guinea-pig hippocampal slice. *J. Physiol.* **461,** 525–547.
44. Traub R. D., Whittington M. A., Colling S. B., Buzsáki G. and Jefferys J. G. R. (1996) Analysis of gamma rhythms in the rat hippocampus *in vitro* and *in vivo*. *J. Physiol.* **493,** 471–484.
45. Traub R. D. and Wong R. K. S. (1982) Cellular mechanism of neuronal synchronization in epilepsy. *Science* **216,** 745–747.
46. Traub R. D. and Wong R. K. S. (1983) Synaptic mechanisms underlying interictal spike initiation in a hippocampal network. *Neurology* **33,** 257–266.
47. Valiante T. A., Perez Velazquez J. L., Jahromi S. S. and Carlen P. L. (1995) Coupling potentials in CA1 neurons during calcium-free-induced field burst activity. *J. Neurosci.* **15,** 6946–6956.
48. Vaney D. I. (1993) The coupling pattern of axon-bearing horizontal cells in the mammalian retina. *Proc. R. Soc. Lond. B* **252,** 93–101.
49. Wong R. K. S. and Traub R. D. (1983) Synchronized burst discharge in disinhibited hippocampal slice. I. Initiation in CA2–CA3 region. *J. Neurophysiol.* **49,** 442–458.
50. Yang X.-D., Korn H. and Faber D. S. (1990) Long-term potentiation of electrotonic coupling at mixed synapses. *Nature* **348,** 542–545.
51. Yasargil G. M. and Sandri C. (1990) Topography and ultrastructure of commissural interneurons that may establish reciprocal inhibitory connections of the Mauthner axons in the spinal cord of the tench, *Tinca tinca* L. *J. Neurocytol.* **19,** 111–126.
52. Ylinen A., Bragin A., Nádasdy Z., Jandó G., Szabó I., Sik A. and Buzsáki G. (1995) Sharp wave-associated high-frequency oscillaiton (200 Hz) in the intact hippocampus: network and intracellular mechanisms. *J. Neurosci.* **15,** 30–46.

(*Accepted* 16 *December* 1998)

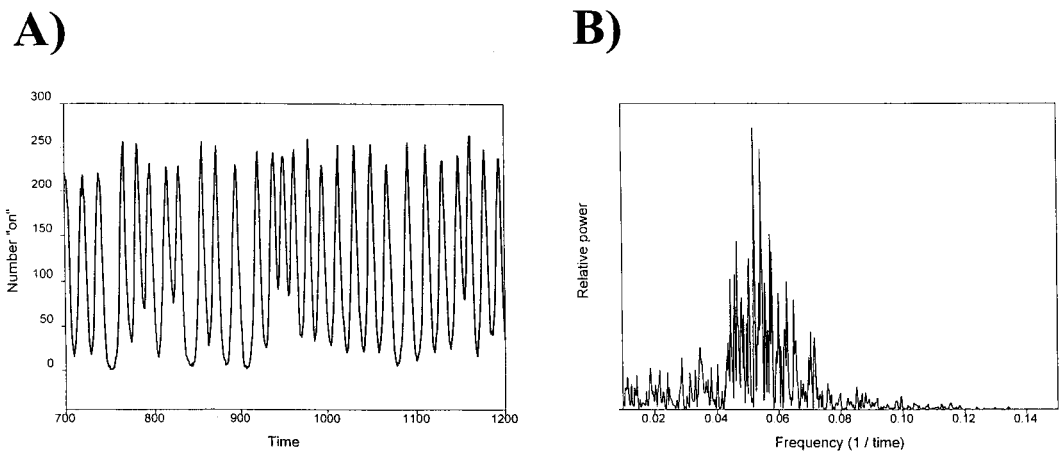

Fig. 15. Rhythmic behaviour in the cellular automaton model. (A) Plot of number of cells "on" as a function of time, showing a rhythmic pattern. (B) Power spectrum of 4096 points of the signal shown, in part, in A. Parameters: 3072 cells total; 2500 junctions total (hence $j = 5000/3072 = 1.63$; $c = j/2 = 0.81$); three refractory states ($r = 3$); λ (mean interval between spontaneous inputs in each cell) = 4000 time steps.

APPENDIX. A CELLULAR AUTOMATON MODEL OF OSCILLATIONS IN SPARSE RANDOM NETWORKS

In this section, we describe an attempt to capture—in as simple a fashion as possible—the basic physical principles of a collection of neurons, interconnected by axoaxonal gap junctions, in which spike propagation from axon to axon is possible.

The most critical elements in the "full" model are: (i) the axonal compartment at the site of the gap junctions, a unit which can "fire" or "not fire"; and (ii) the gap junctions themselves, which we assume are able to conduct spikes faithfully, in the absence of axonal membrane refractoriness. It is these two elements, and these alone, which will be represented in the cellular automaton model. The soma/dendritic portions of the cells, of course, also contribute to network behaviour with: (i) long-lasting AHPs, that sculpt the high-frequency oscillations into transient epochs usually lasting only some hundreds of milliseconds or less (hence, the reduced model—lacking AHPs—is expected to oscillate either continuously or not at all); and (ii) reflected spikes, whose contribution will be lost in the cellular automaton model.

The structure of the cellular automaton model is then as follows:

1. There are n "cells" (each actually representing a bit of axon), interconnected randomly by N "bonds" or "junctions" (see Experimental Procedures).[10] In the notation used earlier, $c = N/n$.
2. Each "cell" has a finite number of states: "on"; a number of refractory states, $refr_1$, $refr_2$, …, $refr_r$, where r is a parameter; and "excitable". Time is discrete.
3. Each "cell" receives random "ectopic" inputs, as an independent Poisson process, with parameter λ, the "mean interval between spontaneous inputs in each cell".
4. Every time step, the states of all of the "cells" are updated by these rules:

$on \rightarrow refr_1$
$refr_1 \rightarrow refr_2$
(etc.)
$refr_{r-1} \rightarrow refr_r$
$refr_r \rightarrow excitable$
$excitable \rightarrow on$, if the cell is receiving a spontaneous input
$excitable \rightarrow on$, if at least one of the cell's inputs is "on"
$excitable \rightarrow excitable$, otherwise.

The model, then, has only four parameters: n, N, r and λ. The time step can be thought of as the duration of an axonal spike, a fraction of a millisecond. r is usually taken as 3.

What is remarkable is that this simple model produces rhythmic waves of activity, provided that $r > 1$ (otherwise the cells in the big cluster turn on and then most of them are continually re-excited, so that the wave cannot terminate). That one "ectopic" event will lead to firing of much of the population is straightforward, as interactions between cells are all excitatory and all-or-none. What is not straightforward is that the wave of activity will shut off, to be succeeded later by another wave, after a time longer than r time steps. This shutting off of the waves, and initiation of new waves, requires two additional constraints on the parameters: (i) λ cannot be too small (otherwise, background activity will keep most of the cells on continuously); and (ii) N cannot be too large, for if there are too many connections (and r is small, say 3 or 4), then cells that are "on" at the beginning of a wave will—with high probability—be excited by cells "on" toward the end of the wave, preventing the system from oscillating. Parameters for which the system can oscillate are comparable to those used to produce oscillations in the "detailed" model in the body of this paper.

Some properties of the cellular automaton model are illustrated next. Figure 15A shows the "oscillatory" behaviour of the system, when the number of cells "on" is plotted as a function of time. [In fact, the complicated power spectrum (Fig. 15B) shows that the system is not oscillating in a precise mathematical sense, but the behaviour is "rhythmic".] The mean period of this signal is about 20 time steps, much longer than the refractory period (three time steps). This system has the same size (3072 cells) as for the detailed model.

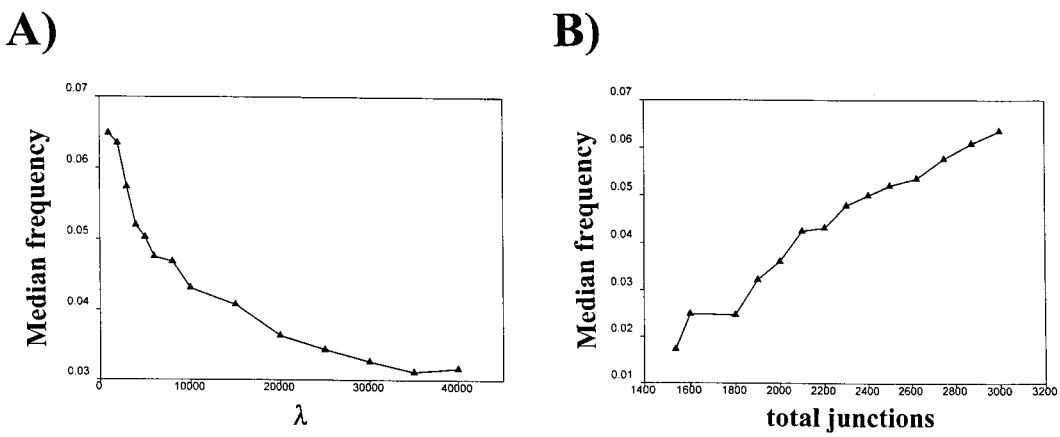

Fig. 16. Cellular automaton model: dependence of frequency on parameters. (A) Median frequency (in the band $0.01–0.15\Delta t^{-1}$) as a function of the background noise parameter λ (mean interval between spontaneous events in each cell). Parameters: 3072 cells; 5000 junctions; three refractory states ($r = 3$). (B) Median frequency (in the band $0.01–0.15\Delta t^{-1}$) as a function of the total number of junctions N in the network. Parameters: 3072 cells; three refractory states; $\lambda = 4000$ time steps.

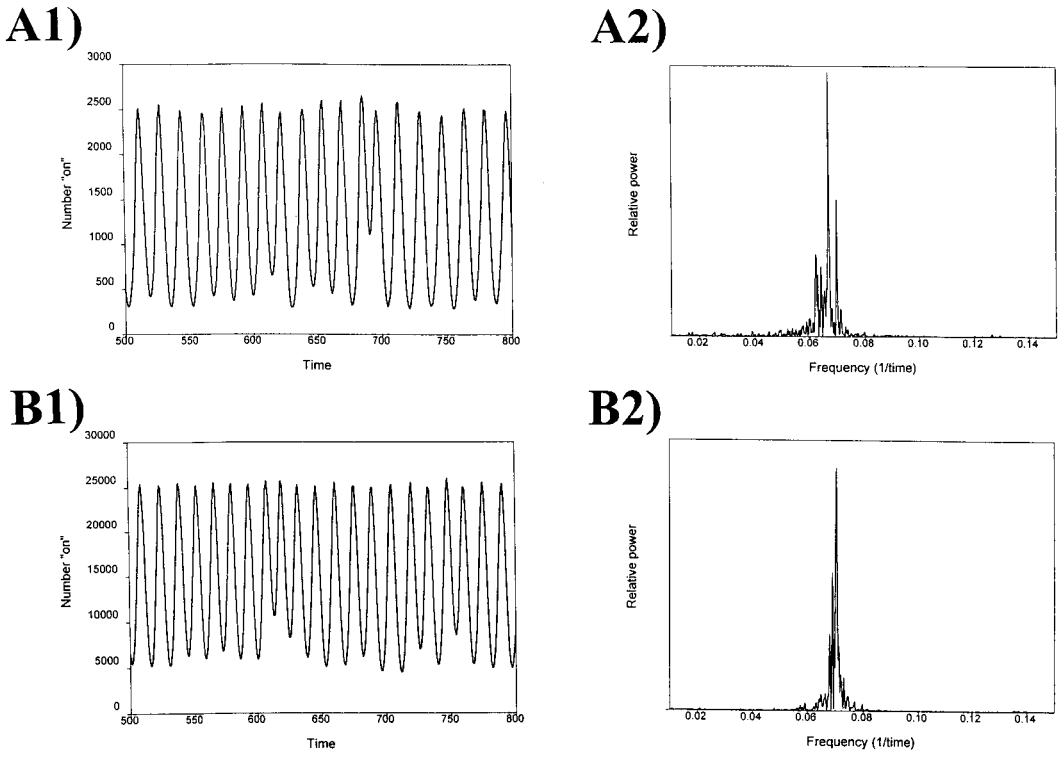

Fig. 17. Cellular automaton model: scale invariance of the oscillation. The network can generate oscillations of similar frequency when the number of cells varies over at least two orders of magnitude (compare Fig. 15), when (no. of junctions)/(no. of cells) remains constant (at about 5/6) and λ also remains constant (4000 time steps). (A) Thirty thousand cells. (A1) Number of cells "on" as a function of time. (A2) Power spectrum of this signal (4096 time steps). (B) Three hundred thousand cells. (B1) Number of cells "on" as a function of time. (B2) Power spectrum of this signal (4096 time steps). In each case, $r = 3$ (model cells have three refractory states).

Figure 16 illustrates the effects on frequency of some parameter changes. Figure 16A shows that a 40-fold increase in λ leads to about a twofold decrease in frequency, while Fig. 16B shows the rise in frequency as connectivity (N, the total number of bonds) is increased. Of course, if N is too small, there is no large cluster, and oscillations will be hard to observe in the total number of cells "on". On the other hand, if N is too large, the system cannot oscillate, as discussed above. Note that, as N decreases, the mean path length on the large cluster will increase (as shown by direct calculation; not illustrated). Thus, Fig. 16B implies that a reduction in path length, in a network of fixed size and with ectopic spike rate fixed, will increase the oscillation frequency; this result is in accord with the analysis of Fig. 11, at least qualitatively. Oscillation amplitude also decreases as N is reduced, owing to the fact that the size of the large cluster depends monotonically on N (Fig. 3).

Finally, Fig. 17 shows that, with constant λ, N/n and r, the oscillation pattern is independent of n, i.e. independent of network size. This important result indicates that, if a sparse network of axoaxonally coupled cells (with less than two gap junctions on each axon, on average) accounts for high-frequency oscillations *in vitro*, then the same mechanism—with the same low density of connections—could account for high-frequency oscillations *in vivo*.